
Incremental Learning in Transformers for In-Context Associative Recall

Anonymous Author(s)

Affiliation
Address
email

Abstract

1 Transformers acquire in-context learning abilities in abrupt phases during training,
2 often unfolding over multiple stages, during which certain keys circuits like induc-
3 tion heads emerge. In this work, we characterize the training dynamics behind the
4 emergence of such circuits during these stages. We focus on a synthetic in-context
5 associative recall task, where sequences are drawn from random maps between a
6 permutation group and a vocabulary range and the model is required to complete
7 the mapping of a permutation by retrieving it from the context. On this task, we
8 study the trajectories of gradient flow of a simplified two-layer, attention-only
9 transformer. Leveraging symmetries in both the transformer architecture and the
10 data, we derive conservation laws that guide the dynamics of the parameters. These
11 conservation laws crucially reveal how initialization —both in shape and scale—
12 determines the order of learning as well as the timescales over which such circuits
13 emerge revealing the implicit curriculum. Furthermore, at the limit of vanishing
14 scale of initialization, we characterize the trajectory of the gradient flow revealing
15 how the training jumps from one saddle to another.

16 1 Introduction

17 In-context learning (ICL) [11], the ability of a model to perform new tasks from examples provided
18 in its prompt without parameter updates, is a characteristic ability of language models. Beyond what
19 these models can do in context, how these abilities emerge during training remains poorly understood.
20 Empirical works [30, 12] report long plateaus in the training loss followed by abrupt transitions, after
21 which specific circuits, such as induction heads, become functional. Understanding these training
22 dynamics is essential both for theory (which optimization biases make ICL learnable by gradient
23 descent) and for practice (how hyperparameters impact convergence speed and training stability).

24 While recent analyses [28, 13] have advanced understanding, they fall short of a complete explanation.
25 Approaches based on layerwise training [28] or highly simplified architectures [41] (e.g., linear
26 attentions) have crucially clarified isolated aspects of the phenomenon, but struggle to account for the
27 sequential acquisition of partial solutions and the duration of plateau phases observed in full models.
28 In particular, we lack a theory that predicts the order in which partial circuits appear, and that explains
29 what controls the length of each phase, including sensitivity to initialization scale.

30 In this paper, we propose combining optimization dynamics with mechanistic interpretability to
31 study how circuits emerge during training. Our analysis is purely dynamical, we study the training
32 trajectories induced by gradient-based optimization, yet our conclusions are mechanistic: we identify
33 which circuit is implemented, which sub-circuits appear first, and how the full circuit crystallizes.

34 To render the problem analytically tractable while preserving its essential structure, we introduce a
35 simplified recall task that retains the induction mechanism underlying in-context n-gram learning
36 but in a form that is more amenable to analysis. Crucially, we couple this task with a series of

37 principled simplifications, that isolate the essential components of the transformer responsible for
 38 incremental learning, while removing spurious elements that obscure analysis. Our analysis reveals a
 39 staged learning process: training trajectories encounter intermediate, partially correct solutions where
 40 gradients nearly vanish (training plateaus) before transitioning to higher-order solutions.

41 **Contributions.** Our results (i) formalize a in-context recall task that preserves the induction structure
 42 while enabling tractable analysis, (ii) derive training dynamics that exhibit plateaus aligned with sub-
 43 circuits, and (iii) provide quantitative predictions for phase ordering and lengths as functions of model
 44 and optimization parameters, with empirical validation on small transformers trained end-to-end.

45 2 Problem Setting

46 2.1 In-Context Associative Recall Task

47 In-context learning abilities of transformers are driven by certain key circuits, such as induction heads.
 48 A basic induction head circuit [30] learns to complete simple repeating patterns, e.g., $[A][B][C] \dots [A]$.
 49 When the model encounters the second $[A]$, the circuit attends to the first $[A]$ and predicts the
 50 subsequent token, $[B]$. This paper investigates how models handle a more general version of this
 51 pattern: $[A][B][C][X] \dots [A][B][C]$. In this setting, the model must recognize the entire sequence
 52 $[A][B][C]$, locate its previous occurrence in the context, and then use it to predict the next token $[X]$.
 53 Formally, the task is defined as follows. The model must complete a sequence by matching the last k
 54 tokens, where $k > 1$ is the *task order*. Let \mathcal{P}_k denote the set of all permutations of $\{0, 1, \dots, k-1\}$,
 55 indexed as $\pi_1, \pi_2, \dots, \pi_{k!}$, where each π_i is a string of k numbers. Let \mathcal{R} be the set of possible
 56 responses. The task is defined by a function $f : \mathcal{P}_k \rightarrow \mathcal{R}$, sampled from a uniform distribution $\mathcal{D}(\mathcal{F})$
 57 over the set of all such functions $\mathcal{F} = \{f \mid f : \mathcal{P}_k \rightarrow \mathcal{R}\}$. An input sequence is then generated by
 58 first sampling $q \in \mathcal{P}_k$ uniformly at random, and independently sampling a function f_τ from $\mathcal{D}(\mathcal{F})$.
 59 The final input sequence takes the form:

$$\underbrace{\pi_{(1,0)}, \pi_{(1,1)}, \dots, \pi_{(1,k-1)}, f_\tau(\pi_1)}_{\pi_1}, \underbrace{\pi_{(2,0)}, \dots, \pi_{(2,k-1)}, f_\tau(\pi_2)}_{\pi_2}, \dots, \underbrace{q_0, \dots, q_{k-1}, ?}_{q_{M-1}}$$

60 Note that π_1, π_2, \dots each represent a sequence of k tokens, rather than a single token. For example,
 61 $\pi_1 = 0, 1, \dots, k-1$. Figure ?? illustrates the task for $k = 2$ with a response set $\{A, B\}$. We define
 62 the vocabulary as $\mathcal{S} = [k] \cup \mathcal{R}$. Each sequence has a fixed length of $l = (k+1)! + k$. To solve this
 63 task, the transformer must learn to identify the part of the context that matches the final k tokens and
 64 recall the subsequent token. For completeness, the context contains all possible query permutations,
 65 ensuring that the model can always retrieve the correct response, which enables exact learning.

66 2.2 Multi-headed Attention-Only Transformer

67 We analyze a specific attention-only transformer with a two-layer structure. The first layer contains
 68 k attention heads, and the second layer contains a single head. The architecture is based on the
 69 disentangled transformer [15, 28] and incorporates several simplifications from prior work [28, 14].

70 **Token encodings.** We represent the input sequence using one-hot encodings. A sequence of length l
 71 is mapped into $\mathbb{R}^{|\mathcal{S}|}$ by the embedding function $E : \mathcal{S} \rightarrow \mathbb{R}^{|\mathcal{S}|}$, defined as $E(i) = \mathbf{e}_i^{|\mathcal{S}|}$ for $i \in [k]$
 72 and $E(r_i) = \mathbf{e}_{k+i}^{|\mathcal{S}|}$. For convenience, we omit the superscript $|\mathcal{S}|$ in what follows. After the encoding
 73 layer, the input sequence x_0, x_1, \dots, x_{l-1} is given by

$$\mathbf{X} = [e_{x_0} \ e_{x_1} \ \dots \ e_{x_{l-1}}]^\top \in \mathbb{R}^{l \times |\mathcal{S}|}.$$

74 **First attention layer.** The first attention layer has k heads and considers only positional information,
 75 which is a convenient choice for this task. We use relative positional encodings with a causal mask.
 76 Each head i is parameterized by a vector $\mathbf{w}^i \in \mathbb{R}^l$. The pre-softmax attention scores of head i form a
 77 lower-triangular matrix with entries given by

$$\mathbf{A}^i[g, h] = \begin{cases} \mathbf{w}_{g-h}^i & \text{if } 0 \leq h \leq g \leq l-1 \\ -\infty & \text{otherwise} \end{cases}. \quad (1)$$

78 The output of attention head i ($1 \leq i \leq k$) is $\mathbf{R}^i = \sigma(\mathbf{A}^i) \mathbf{X} \in \mathbb{R}^{l \times |\mathcal{S}|}$, where σ denotes the
 79 row-wise softmax operation with causal masking. The output of the first attention layer is the

80 concatenation of the outputs from all heads together with a skip connection $\mathbf{R}^0 = \mathbf{X}$ (which differs
 81 from the standard architecture): $\mathbf{R} = [\mathbf{R}^0 \quad \mathbf{R}^1 \quad \dots \quad \mathbf{R}^k] \in \mathbb{R}^{l \times (k+1)|\mathcal{S}|} = \sum_{i=0}^k (\mathbf{e}_i^{k+1})^\top \otimes \mathbf{R}^i$.

Second attention layer. The second attention layer consists of a single head, parameterized by matrices $\mathbf{Q}, \mathbf{K} \in \mathbb{R}^{(k+1)|\mathcal{S}| \times (k+1)|\mathcal{S}|}$. The attention scores are $\sigma(\mathbf{X}\mathbf{Q}^\top \mathbf{K}\mathbf{X}^\top)$, where the softmax is applied row-wise with causal masking. The output of the second layer is $\mathbf{R}_+ = \sigma(\mathbf{R}\mathbf{Q}^\top \mathbf{K}\mathbf{R}^\top) \mathbf{R}V$. We further simplify it by introducing a parameter $\beta \in \mathbb{R}^k$ and parameterize $\mathbf{Q}^\top \mathbf{K}$ as

$$\mathbf{Q}^\top \mathbf{K} = \text{diag}_{-1}(\beta^2) \otimes \tilde{\mathbf{I}}_k, \quad \mathbf{R}_+ = \sigma\left(\mathbf{R} \left[\text{diag}_{-1}(\beta^2) \otimes \tilde{\mathbf{I}}_k \right] \mathbf{R}^\top\right) \mathbf{R}V$$

82 where $\text{diag}_{-1}(u) \in \mathbb{R}^{(k+1) \times (k+1)}$ denotes a matrix with u on its first sub-diagonal and zeros
 83 elsewhere. Squaring of β serves two purposes, (i) it ensures positivity of the entries and (ii) it
 84 preserves the 2-homogeneity of $\mathbf{Q}^\top \mathbf{K}$. We choose the value matrix $V = \mathbf{e}_0^{k+1} \otimes \mathbf{I}_{|\mathcal{S}|} \in \mathbb{R}^{(k+1)|\mathcal{S}| \times |\mathcal{S}|}$.
 85 This matrix consists of a column of blocks, with the identity matrix as the first block and zeros
 86 elsewhere. By construction, V extracts the skip connection from the concatenated output of the first
 87 layer, i.e., $\mathbf{R}V = \mathbf{R}^0 = \mathbf{X}$, using the mixed-product property of the Kronecker product.

88 **The model output.** As the loss is computed only on the *last token*, the model's output depends only
 89 on the embedding of the final token after the second layer, i.e.,

$$\mathbf{p} = (\mathbf{R}_+)_l = (\sigma(\mathbf{R}\mathbf{Q}^\top \mathbf{K}\mathbf{R}^\top) \mathbf{X})_l = \mathbf{R}^\top \left(\sigma(\mathbf{R}\mathbf{Q}^\top \mathbf{K}\mathbf{R}^\top)_l \right) = \mathbf{R}^\top \sigma\left(\left(\mathbf{R}\mathbf{Q}^\top \mathbf{K}\mathbf{R}^\top\right)_l\right).$$

90 We denote the attention scores by $\mathbf{s} = \sigma(\mathbf{R}\mathbf{Q}^\top \mathbf{K}\mathbf{R}^\top)_l$ and the corresponding pre-softmax scores
 91 by $\tilde{\mathbf{s}} = (\mathbf{R}\mathbf{Q}^\top \mathbf{K}\mathbf{R}^\top)_l$. The choice of V together with the orthogonal embeddings ensures that
 92 \mathbf{p} is a valid probability distribution over the vocabulary, i.e., $\mathbf{p} \in \Delta^{|\mathcal{S}|}$, and requires no further
 93 normalization. Hence, the output of the model is given by $\mathbf{p} = \mathbf{X}^\top \mathbf{s} = \mathbf{X}^\top \sigma(\tilde{\mathbf{s}})$. Finally, we denote
 94 the parameters of the simplified model by $\theta = (\mathbf{w}^1, \mathbf{w}^2, \dots, \mathbf{w}^k, \beta)$ here $\mathbf{w}^i \in \mathbb{R}^k$ for all i and
 95 $\beta = (\beta_1, \beta_2, \dots, \beta_k) \in \mathbb{R}^k$. We use $\mathbf{p}(\theta)$ to denote the output of the model for parameters θ . We
 96 refer to section A.2 for a discussion on the simplifications and their implications.

97 2.3 The final problem setup

98 **Training Objective.** We replace the cross-entropy (CE) loss with the dot-product (DP) loss

$$\ell(\mathbf{p}, \mathbf{p}_*) = 1 - \langle \mathbf{p}, \mathbf{p}_* \rangle \quad \ell_{\text{CE}}(\mathbf{p}, \mathbf{p}_*) = -\langle \mathbf{p}_*, \log \mathbf{p} \rangle.$$

99 See App. A.3 for a detailed comparison of the two loss functions. Finally, the population DP loss is

$$\mathcal{L}(\theta) = \mathbb{E}_{f_\tau \sim \mathcal{D}(\mathcal{F}), q \sim \mathcal{P}_k} \ell(\mathbf{p}(\theta), e_{f_\tau(q)}) = 1 - \mathbb{E}_{f_\tau, q} \langle \mathbf{p}(\theta), e_{f_\tau(q)} \rangle. \quad (2)$$

100 **Gradient Flow.** To analyse the training dynamics, we consider the continuous-time limit of gradient
 101 descent, known as gradient flow. The parameters evolve according to the negative gradient of the
 102 population loss \mathcal{L} with respect to the parameters. This approach does not account for the stochasticity
 103 or adaptive features of the optimizers used in practice. Nevertheless, it captures key aspects of
 104 training. The gradient flow is given by

$$\dot{\beta}_h = -\frac{\partial \mathcal{L}}{\partial \beta_h}, \quad \text{and} \quad \dot{\mathbf{w}}_i^h = -\frac{\partial \mathcal{L}}{\partial \mathbf{w}_i^h}, \quad \text{for all } i, h \in [k].$$

105 3 Technical Results

106 **A stagewise learning process.** We train the simplified transformer model with SGD and momentum
 107 on the DP loss over the in-context learning task of order $k+1$. A crucial observation is that the training
 108 dynamics are stage-wise. The model plateaus for an extended period before abruptly transitioning to
 109 another plateau with lower loss, and eventually converges to zero loss. This behavior becomes more
 110 pronounced as the initialization scale decreases, a phenomenon reminiscent of the saddle-to-saddle
 111 dynamics observed in deep networks under small-scale initialization [20, 31].

112 To mechanistically interpret these intermediate stages, we analyze what the model represents on each
 113 plateau, see Figure 1. At the first plateau, the model learns to match a single token in the context:

114 one attention head h_1 and its associated coefficient β_{h_1} are activated. At the second plateau, an
 115 additional head h_2 with coefficient β_{h_2} is activated, enabling the model to match two tokens of the
 116 query, q_{k+1-h_1}, q_{k+1-h_2} in the context. This process continues incrementally: at each stage, a new
 117 head-coefficient pair is activated, allowing the model to match one additional token. After k such
 118 stages, all tokens in the query are matched and the model achieves zero loss. We now turn to a
 119 detailed study of the stage-wise dynamics. We begin by analyzing a stylized initialization that isolates
 120 the transitions between plateaus. We then combine these analyses to obtain a complete picture.

121 **The first jump.** We study the dynamics of the first jump, when the model escapes from the initial
 122 plateau. We consider a stylized initialization, denoted \mathcal{I}_1 , where $\beta_1 = \epsilon$ and $\beta_j = 0$ for all $j \neq 1$.
 123 The heads are initialized as $\mathbf{w}^i = 0$ for all i . Note that at initialization, all heads are symmetric.

124 **Theorem 3.1.** *Consider the simplified transformer model $\theta = (\mathbf{w}^1, \mathbf{w}^2, \dots, \mathbf{w}^k, \beta)$ with k heads and
 125 initialization \mathcal{I}_1 , evolving under gradient flow on the DP loss. Then:*

126 (a) **Directional bias:** For all time $t \geq 0$, $\mathbf{w}^1(t) = \alpha_1(t)\mathbf{e}_1^k + \delta_1(t)\mathbf{1}$ for some $\alpha(t), \delta(t) \in \mathbb{R}$.

127 (b) **Sparse attention:** $\dot{\mathbf{w}}_1^1 > 0$ and $\dot{\mathbf{w}}_i^1 < 0, \forall i \neq 1$, i.e., the head attends to the 1st token from end.

128 (c) **A Sufficient ODE:** The learning dynamics can be fully described by the evolution of $\alpha_1(t), \beta_1(t)$

$$\dot{\alpha}_1 = \frac{\beta_1^2 e^{\alpha_1}}{(e^{\alpha_1} + k - 1)^2} \frac{k^2}{k - 1} \Xi, \quad \dot{\beta}_1 = 2\beta_1 \frac{e^{\alpha_1} - 1}{e^{\alpha_1} + k - 1} \Xi$$

129 where Ξ is defined in equation (4) in Appendix.

130 (d) **Conservation law:** The quantity $f(\alpha_1) - \beta_1^2/4$ is conserved along the trajectory, i.e., the time
 131 derivative $d(f(\alpha_1) - \beta_1^2/4) = 0$ where

$$f(\alpha_1) = 2\frac{k-1}{k^2} (\sinh(\alpha_1) - \alpha_1) - \frac{k-1}{k} [e^{-\alpha_1} + \alpha_1 - 1].$$

132 Some comments are in order. The parameters of the heads except head 1 are stationary. All relative
 133 position encodings except \mathbf{w}_1^1 evolves together. This follows from the inherent symmetry of the task:
 134 since token positions can be permuted within a sequence without leaving the distribution, the dynamics
 135 must preserve this symmetry. Combined with the symmetry of the initialization, this leads to the
 136 directional bias described above. The transformer rapidly learns to attend to the first token and results
 137 in sparse attention. There is a clear dichotomy: the embedding corresponding to this token grows,
 138 while the others decay at proportional rates.

139 From the ODE description, on any compact set, the time derivatives are bounded away from zero,
 140 ensuring that both α_1 and β_1 diverge to infinity, where the gradient is zero. The conservation
 141 law show a coupled evolution of the parameters, note that sub conservation laws are common in
 142 dynamical systems, and recent works have identified conservation principles in transformers as
 143 well [27]. However, prior results are typically restricted to a single attention layer. In contrast,
 144 our result shows how parameters across multiple layers, separated by the softmax, jointly obey a
 145 conservation law.

146 This conservation law allows us to derive the timescale of the jump, i.e., how long training remains in
 147 the plateau. Suppose $\beta_1(0) = \epsilon$ with $\epsilon \approx 0$. For convenience define $s = e^{\alpha_1} - 1$ with $s(0) = 0$, for
 148 small s , a Taylor expansion gives $\beta_1^2 \approx 4s^2 + \epsilon^2$, and the local dynamics reduce to $ds \sim c(s^2 + \epsilon^2)$.
 149 Thus the growth of parameters in self-attention has an information exponent of 2 [5]. Solving the ODE
 150 yields $s \approx \epsilon \tan(\epsilon T)$, implying that s requires $O(1/\epsilon)$ time to reach $O(1)$. When s has sufficiently
 151 grown, the dynamics switch regimes. Now $\beta_h \sim \sqrt{s}, \Xi$ which decays in s kicks in and the ODE
 152 simplifies to

$$ds \sim bse^{-s} \implies \int \frac{e^s}{s} ds = bT \tag{3}$$

153 The integral function on the right-hand side is the exponential integral, implying that s grows at rate
 154 $\log T$ and hence α_1 grows only at rate $\log \log T$.

155 **Full stagewise dynamics.** We refer to Appendix A.6 for the analysis of subsequent jumps, which is
 156 very similar to the first jump but of reduced order. Combining these analyses, we paint a complete
 157 picture of the stagewise dynamics.

158 **References**

159 [1] E. Abbe, E. B. Adsera, and T. Misiakiewicz. Sgd learning on neural networks: leap complexity
160 and saddle-to-saddle dynamics. In *The Thirty Sixth Annual Conference on Learning Theory*,
161 pages 2552–2623. PMLR, 2023.

162 [2] K. Ahn, X. Cheng, H. Daneshmand, and S. Sra. Transformers learn to implement preconditioned
163 gradient descent for in-context learning. *Advances in Neural Information Processing Systems*,
164 36, 2024.

165 [3] E. Akyürek, B. Wang, Y. Kim, and J. Andreas. In-context language learning: Arhitectures and
166 algorithms. *arXiv preprint arXiv:2401.12973*, 2024.

167 [4] S. Arora, N. Cohen, W. Hu, and Y. Luo. Implicit regularization in deep matrix factorization.
168 *Advances in Neural Information Processing Systems*, 32, 2019.

169 [5] G. B. Arous, R. Gheissari, and A. Jagannath. Online stochastic gradient descent on non-convex
170 losses from high-dimensional inference. *Journal of Machine Learning Research*, 22(106):1–51,
171 2021. URL <http://jmlr.org/papers/v22/20-1288.html>.

172 [6] R. Berthier. Incremental learning in diagonal linear networks. *arXiv preprint arXiv:2208.14673*,
173 2022.

174 [7] S. Bhattamishra, A. Patel, P. Blunsom, and V. Kanade. Understanding in-context learning in
175 transformers and llms by learning to learn discrete functions. *arXiv preprint arXiv:2310.03016*,
176 2023.

177 [8] A. Bietti, V. Cabannes, D. Bouchacourt, H. Jegou, and L. Bottou. Birth of a transformer: A
178 memory viewpoint. *Advances in Neural Information Processing Systems*, 36, 2024.

179 [9] E. Boix-Adsera, E. Littwin, E. Abbe, S. Bengio, and J. Susskind. Transformers learn through
180 gradual rank increase. *arXiv preprint arXiv:2306.07042*, 2023.

181 [10] E. Boursier, L. Pillaud-Vivien, and N. Flammarion. Gradient flow dynamics of shallow reLU
182 networks for square loss and orthogonal inputs. In A. H. Oh, A. Agarwal, D. Belgrave, and
183 K. Cho, editors, *Advances in Neural Information Processing Systems*, 2022. URL <https://openreview.net/forum?id=L74c-iUxQ1I>.

185 [11] T. B. Brown. Language models are few-shot learners. *arXiv preprint arXiv:2005.14165*, 2020.

186 [12] A. Chen, R. Shwartz-Ziv, K. Cho, M. L. Leavitt, and N. Saphra. Sudden drops in the loss:
187 Syntax acquisition, phase transitions, and simplicity bias in MLMs. In *The Twelfth International
188 Conference on Learning Representations*, 2024. URL <https://openreview.net/forum?id=M05PiKHELW>.

190 [13] S. Chen, H. Sheen, T. Wang, and Z. Yang. Unveiling induction heads: Provable training
191 dynamics and feature learning in transformers. In *The Thirty-eighth Annual Conference on
192 Neural Information Processing Systems*, 2024.

193 [14] B. L. Edelman, E. Edelman, S. Goel, E. Malach, and N. Tsilivis. The evolution of statistical
194 induction heads: In-context learning markov chains. *arXiv preprint arXiv:2402.11004*, 2024.

195 [15] D. Friedman, A. Wettig, and D. Chen. Learning transformer programs. In *Thirty-seventh
196 Conference on Neural Information Processing Systems*, 2023.

197 [16] K. Fukumizu and S. Amari. Local minima and plateaus in hierarchical structures of multilayer
198 perceptrons. *Neural Networks*, 13(3):317–327, 2000. ISSN 0893-6080. doi: [https://doi.org/10.1016/S0893-6080\(00\)00009-5](https://doi.org/10.1016/S0893-6080(00)00009-5). URL <https://www.sciencedirect.com/science/article/pii/S0893608000000095>.

201 [17] S. Garg, D. Tsipras, P. S. Liang, and G. Valiant. What can transformers learn in-context? a
202 case study of simple function classes. *Advances in Neural Information Processing Systems*, 35:
203 30583–30598, 2022.

204 [18] G. Gidel, F. Bach, and S. Lacoste-Julien. Implicit regularization of discrete gradient dynamics
205 in linear neural networks. *Advances in Neural Information Processing Systems*, 32, 2019.

206 [19] D. Gissin, S. Shalev-Shwartz, and A. Daniely. The implicit bias of depth: How incremental
207 learning drives generalization. In *International Conference on Learning Representations*, 2020.

208 [20] A. Jacot, F. Ged, B. Şimşek, C. Hongler, and F. Gabriel. Saddle-to-saddle dynamics in
209 deep linear networks: Small initialization training, symmetry, and sparsity. *arXiv preprint*
210 *arXiv:2106.15933*, 2021.

211 [21] L. Jiang, Y. Chen, and L. Ding. Algorithmic regularization in model-free overparametrized
212 asymmetric matrix factorization. *arXiv preprint arXiv:2203.02839*, 2022.

213 [22] J. Jin, Z. Li, K. Lyu, S. S. Du, and J. D. Lee. Understanding incremental learning of gradient
214 descent: A fine-grained analysis of matrix sensing. *arXiv preprint arXiv:2301.11500*, 2023.

215 [23] D. Jurafsky and J. H. Martin. *Speech and Language Processing: An Introduction to Natural*
216 *Language Processing, Computational Linguistics, and Speech Recognition*. Prentice Hall,
217 Upper Saddle River, NJ, 2nd edition, 2009.

218 [24] J. Kim, S. Kwon, J. Y. Choi, J. Park, J. Cho, J. D. Lee, and E. K. Ryu. Task diversity shortens
219 the icl plateau, 2024. URL <https://arxiv.org/abs/2410.05448>.

220 [25] Z. Li, Y. Luo, and K. Lyu. Towards resolving the implicit bias of gradient descent for matrix fac-
221 torization: Greedy low-rank learning. In *International Conference on Learning Representations*,
222 2021.

223 [26] A. V. Makkluva, M. Bondaschi, A. Girish, A. Nagle, M. Jaggi, H. Kim, and M. Gastpar. Attention
224 with markov: A framework for principled analysis of transformers via markov chains. *arXiv*
225 *preprint arXiv:2402.04161*, 2024.

226 [27] S. Marcotte, R. Gribonval, and G. Peyré. Transformative or conservative? conservation laws for
227 resnets and transformers. *arXiv preprint arXiv:2506.06194*, 2025.

228 [28] E. Nichani, A. Damian, and J. D. Lee. How transformers learn causal structure with gradient
229 descent, 2024. URL <https://arxiv.org/abs/2402.14735>.

230 [29] E. Nichani, J. D. Lee, and A. Bietti. Understanding factual recall in transformers via associative
231 memories. In *The Thirteenth International Conference on Learning Representations*, 2025.
232 URL <https://openreview.net/forum?id=hwSmPOAmhk>.

233 [30] C. Olsson, N. Elhage, N. Nanda, N. Joseph, N. DasSarma, T. Henighan, B. Mann, A. Askell,
234 Y. Bai, A. Chen, et al. In-context learning and induction heads. *arXiv preprint arXiv:2209.11895*,
235 2022.

236 [31] S. Pesme and N. Flammarion. Saddle-to-saddle dynamics in diagonal linear networks. *Advances*
237 *in Neural Information Processing Systems*, 36:7475–7505, 2023.

238 [32] N. Rajaraman, M. Bondaschi, K. Ramchandran, M. Gastpar, and A. V. Makkluva. Transformers
239 on markov data: Constant depth suffices. *arXiv preprint arXiv:2407.17686*, 2024.

240 [33] N. Razin, A. Maman, and N. Cohen. Implicit regularization in tensor factorization. In *Inter-
241 national Conference on Machine Learning*, pages 8913–8924. PMLR, 2021.

242 [34] A. M. Saxe, J. L. McClelland, and S. Ganguli. A mathematical theory of semantic development
243 in deep neural networks. *Proceedings of the National Academy of Sciences*, 116(23):11537–
244 11546, 2019.

245 [35] C. E. Shannon. A mathematical theory of communication. *The Bell system technical journal*,
246 27(3):379–423, 1948.

247 [36] A. Svete and R. Cotterell. Transformers can represent n -gram language models. *arXiv preprint*
248 *arXiv:2404.14994*, 2024.

249 [37] A. Varre, G. Yüce, and N. Flammarion. Learning in-context n -grams with transformers:
 250 Sub- n -grams are near-stationary points. In *International Conference on Machine Learning*,
 251 2025.

252 [38] A. V. Varre, M.-L. Vladarean, L. Pillaud-Vivien, and N. Flammarion. On the spectral bias of
 253 two-layer linear networks. In *Thirty-seventh Conference on Neural Information Processing
 254 Systems*, 2023. URL <https://openreview.net/forum?id=FFdrXkm3Cz>.

255 [39] A. V. Varre, M. Sagitova, and N. Flammarion. Sgd vs gd: Rank deficiency in linear networks.
 256 *Advances in Neural Information Processing Systems*, 37:60133–60161, 2024.

257 [40] J. Von Oswald, E. Niklasson, E. Randazzo, J. Sacramento, A. Mordvintsev, A. Zhmoginov, and
 258 M. Vladymyrov. Transformers learn in-context by gradient descent. In *International Conference
 259 on Machine Learning*, pages 35151–35174. PMLR, 2023.

260 [41] Y. Zhang, A. K. Singh, P. E. Latham, and A. Saxe. Training dynamics of in-context learning in
 261 linear attention, 2025. URL <https://arxiv.org/abs/2501.16265>.

262 **A Appendix**

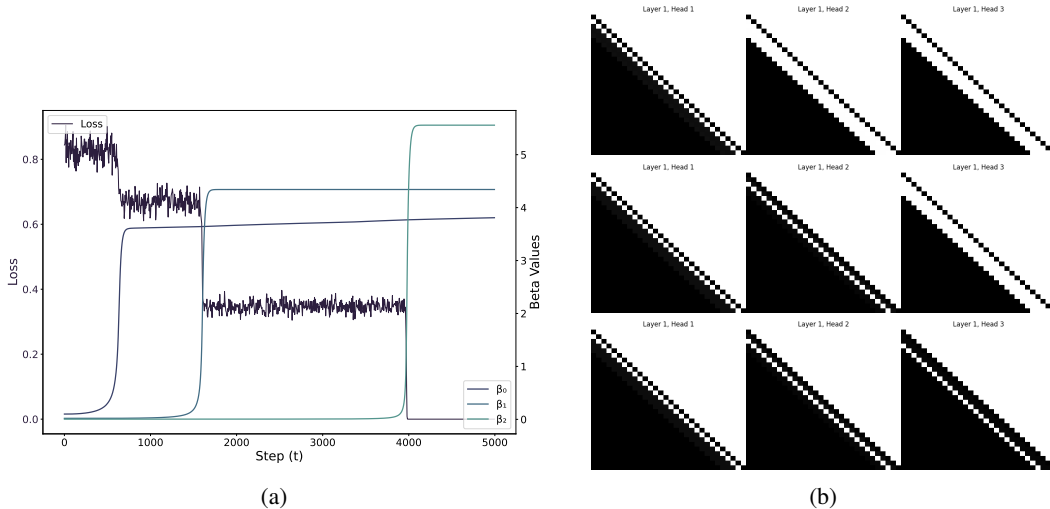


Figure 1: The left panel is shown in **a** and the right panel in **b**. Note that the β values rise simultaneously with the loss, and the attention patterns at times 800, 1750, and 4500 demonstrate incremental learning.

263 **Notation.** For any positive integers a, b, s , $[s]$ denotes the set $\{0, 1, \dots, s - 1\}$, and $[a, b]$ represents
 264 $\{a, \dots, b\}$. For a vector v , its i -th coordinate is v_i and e_i^s is the i -th standard basis vector in \mathbb{R}^s . For a
 265 matrix $A \in \mathbb{R}^{m \times n}$, its entry at row i and column j is A_{ij} , and its r -th row is $A_r \in \mathbb{R}^n$. For any set
 266 S , $|S|$ denotes the cardinality of the vocabulary. Δ^N denotes the probability simplex in \mathbb{R}^N . The
 267 Kronecker product is denoted by \otimes . We use $\mathbf{1}$ to denote all vector of all ones.

268 **Definition A.1** (Jacobian of a function). Let $f : \mathbb{R}^m \rightarrow \mathbb{R}^n$ be a C_1 -function defined on a variable
 269 $X \in \mathbb{R}^m$. $\frac{\partial f}{\partial X}$ denotes the Jacobian which is a function from $\mathbb{R}^m \rightarrow \mathbb{R}^{n \times m}$.

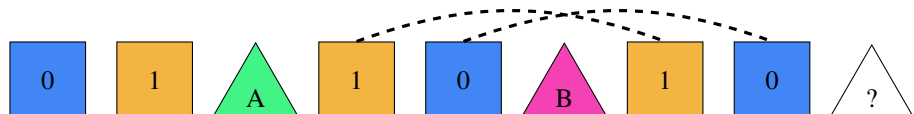


Figure 2: Illustration of the in-context associative recall task. The sequence shows mappings between query permutation elements (rectangles labeled 0, 1) and response tokens (triangles labeled A, B). The model must predict the missing association, marked with "?".

270 **A.1 Related Work**

271 **In-context learning.** The phenomenon of in-context learning (ICL) [11] has been investigated
 272 from several perspectives. Mechanistic interpretability has identified induction heads as key circuits
 273 supporting ICL [30]. A complementary direction examines restricted hypothesis classes, providing
 274 controlled settings to analyze how transformers develop in-context capabilities. A recurring observa-
 275 tion across these studies is the emergence of training plateaus followed by sudden capability gains
 276 [12, 24]. These dynamics have been observed in regression tasks [17, 40, 2], boolean and formal
 277 language recognition [7, 3], and n-gram prediction.

278 **n-gram models.** n-grams models are related our work as the transformer circuit that solves our
 279 task also solves the tasks of in-context learning n-grams. n-gram language models [35, 23] provide a
 280 natural testbed for analyzing transformer behavior. Several recent works adopt this viewpoint: the
 281 optimization landscape has been analyzed in [26], expressivity over n-gram distributions in [36],
 282 and in-context generalization in [32]. Other studies connect ICL to the emergence of induction
 283 heads [8] and their acquisition through gradient descent [28]. Edelman et al. [14] identify stage-wise
 284 dynamics in transformer training on in-context n-gram prediction, where intermediate solutions
 285 resemble sub-n-grams, while Varre et al. [37] formalize these sub-n-grams as near-stationary points.
 286 Finally, Chen et al. [13] investigate the same task with a modified architecture and initialization
 287 scheme that enforces head specialization from the start, thereby eliminating the stage-wise dynamics
 288 central to our analysis.

289 **Incremental learning.** Plateau-shaped learning curves arise broadly in neural network training,
 290 beyond ICL. Early work by Fukumizu and Amari [16] linked such phenomena to critical points
 291 in supervised learning. Related characterizations appear in simplified models such as matrix and
 292 tensor factorization [33, 21], matrix sensing [4, 25, 22], diagonal and linear networks [19, 34, 18, 20,
 293 6, 31, 38, 39], ReLU networks [10, 1], and simplified transformer architectures [9]. Nichani et al.
 294 [29] studied the stage wise dynamics in Factual recall with linear attention. These results provide
 295 theoretical tools that we build on to characterize plateaus in in-context learning.

296 **A.2 A simplified model**

297 The goal of this paper is to study the training dynamics of transformers on the in-context associative
 298 recall task. The simplified architecture described above, although easier than a full transformer,
 299 remains too complex for a complete study of training dynamics. To address this intractability, we
 300 introduce additional simplifications that preserve the qualitative behavior of the full model while
 301 making analysis feasible. Before detailing these simplifications, we first present the construction of
 302 the solution implemented by the transformer for this task, which clarifies the rationale behind our
 303 design choices.

304 **The transformer’s solution.** To solve the task, the transformer must learn to attend to the portion of
 305 the context that matches the final k tokens. This mechanism is implemented through a multi-head
 306 construction, variants of which have appeared in prior work [14, 32]. Its parameters are defined as

$$\mathbf{w}^i = c \cdot \mathbf{e}_i^t \text{ where } i \in [1, k], \quad \mathbf{Q}^\top \mathbf{K} = c \left(\mathbf{B} \otimes \tilde{\mathbf{I}}_k^\top \right).$$

307 Here c is a positive constant, $\tilde{\mathbf{I}}_k \in \mathbb{R}^{|\mathcal{S}| \times |\mathcal{S}|}$ where the first $k \times k$ block is given by $\tilde{\mathbf{I}}_{:k,:k} = \mathbf{I}_k - \gamma \mathbf{1}_k \mathbf{1}_k^\top$
 308 and 0’s elsewhere. The matrix $\mathbf{B} \in \mathbb{R}^{(k+1) \times (k+1)}$ is defined as

$$\text{For } 0 \leq g, h \leq k \quad \mathbf{B}_{gh} = \begin{cases} 1 & \text{if } g+1 = h \\ 0 & \text{otherwise} \end{cases}.$$

As $c \rightarrow \infty$, the relative positional encoding ensures that head h outputs the embedding of x_{i-h} for
 token i . With this choice of \mathbf{B} , the presoftmax attention scores are $\tilde{\mathbf{s}}_i \approx c \sum_{h=1}^k \mathbb{1}\{x_{i-h} = x_{i-h}\}$
 which is maximized when the histories of i and l match. In the limit $c \rightarrow \infty$, the softmax approaches
 hardmax attention, i.e, $\mathbf{s}_i \rightarrow 1$ (where i is the token that matches the history). The model output is
 then

$$\mathbf{p} = \sum_j \mathbf{s}_j e_{x_j} \approx e_{x_i}.$$

309 This construction is illustrated in the Figure 3.

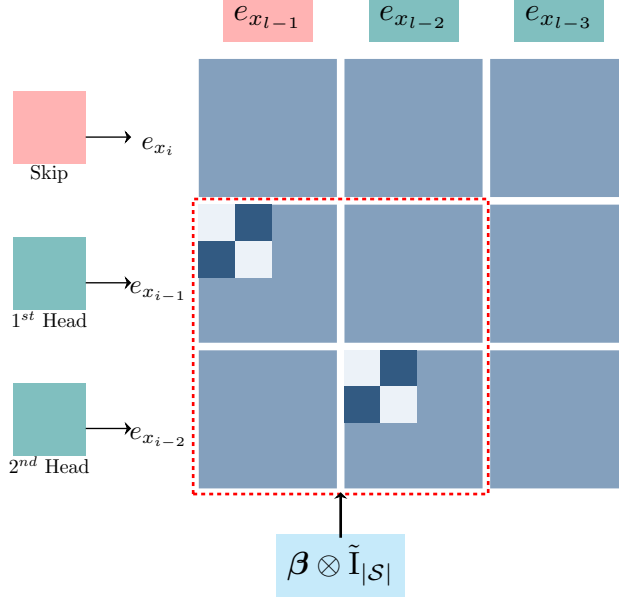


Figure 3: Layer-2 representation structure of the optimal solution constructed by the transformer We use it to simplify this structure by a diagonal block matrix with trainable scales.

310 **Simplifying the model.** Our simplifications are motivated by the transformer’s solution described
 311 above and preserve its overall structure, especially in the second layer. We emphasize that, despite
 312 these simplifications, the analysis remains intricate, as shown in the following sections and the training
 313 dynamics of the simplified model closely mirror those of the original model. For $i \in [k, l-1]$, $t \in [l]$, $h \in [1, k]$, the modification of the parametric model are given by:
 314

	Original model	Simplified model
	$\mathbf{R}_i^h = \sum_{j=0}^i \sigma(\mathbf{A}^h)_{ij} e_{x_j},$	$\mathbf{R}_i^h = \sum_{j=i-k}^{i-1} \sigma(\mathbf{A}^h)_{ij} e_{x_j},$
315	$\tilde{\mathbf{s}}_t = \sum_{g,h=0}^k [\mathbf{R}_{i-1}^h]^\top [\mathbf{Q}^\top \mathbf{K}]_{hg} [\mathbf{R}_t^g],$	$\tilde{\mathbf{s}}_t = \sum_{h=1}^k [e_{x_{l-h}}]^\top \beta_h^2 [\tilde{\mathbf{I}}_k] [\mathbf{R}_t^h],$
	$\mathbf{s} = \sigma(\tilde{\mathbf{s}}), \quad \mathbf{p} = \sum_{t=0}^{l-1} \mathbf{s}_t e_{x_t}.$	$\mathbf{s} = \sigma(\tilde{\mathbf{s}}_{\mathcal{R}}), \quad \mathbf{p} = \sum_{t:x_t \in \mathcal{R}} \mathbf{s}_t e_{x_t}.$

316 In words, we make the following modifications:

317 (A0) We fix the attention window in the first layer to k for all heads. For each head h we train only
 318 the weights \mathbf{w}_j^h for $1 \leq j \leq k$ while the remaining entries are masked out and set to $-\infty$.
 (A1) We configure the second-layer attention parameters to match the structure of the optimal
 solution shown in Figure 3. This configuration is held fixed, and we train only the scalar
 multipliers that scale these parameters. In particular, we introduce a parameter $\beta \in \mathbb{R}^k$ and
 parameterize $\mathbf{Q}^\top \mathbf{K}$ as

$$\mathbf{Q}^\top \mathbf{K} = \text{diag}_{-1}(\beta^2) \otimes \tilde{\mathbf{I}}_k,$$

319 where $\text{diag}_{-1}(u) \in \mathbb{R}^{(k+1) \times (k+1)}$ denotes a matrix with u on its first sub-diagonal and zeros
 320 elsewhere. Squaring of β serves two purposes, (i) it ensures positivity of the entries and (ii) it
 321 preserves the 2-homogeneity of $\mathbf{Q}^\top \mathbf{K}$.

322 (A2) As a further simplification, we replace the embeddings of the last with its embeddings at the
 323 solution. This assumption is mild and does not affect the training dynamics. It is mainly a
 324 convenience, as it avoids the bilinearity of the first layer outputs and leads to simpler gradient
 325 computations.

326 (A3) Since the output always lies in \mathcal{R} , we trim \tilde{s} and apply the softmax only to the coordinates
 327 corresponding to responses. This ensures the output is always a probability vector over \mathcal{R} .

328 Other than (A1) which simplifies the second attention layer from matrix parameters to vector
 329 parameters, the other simplifications are mild and do not affect the essence of the analysis. We justify
 330 these choices both analytically and empirically in the next section.

331 Finally, we denote the parameters of the simplified model by $\theta = (\mathbf{w}^1, \mathbf{w}^2, \dots, \mathbf{w}^k, \beta)$ here $\mathbf{w}^i \in \mathbb{R}^k$
 332 for all i and $\beta = (\beta_1, \beta_2, \dots, \beta_k) \in \mathbb{R}^k$. We use $\mathbf{p}(\theta)$ to denote the output of the model for
 333 parameters θ .

334 **A.3 Cross Entropy and Dot-Product losses.**

335 The minimum of the DP loss is

$$\arg \min_{\mathbf{p} \in \Delta^{|\mathcal{S}|}} 1 - \langle \mathbf{p}, \mathbf{p}_* \rangle = e_i \text{ where } i = \arg \max_j (\mathbf{p}_*)_j,$$

336 while the minimum of the CE loss is \mathbf{p}_* . These minima coincide whenever \mathbf{p}_* is a one-hot vector.
 337 Since in our task each input sequence has a unique correct response, the target distribution \mathbf{p}_* is
 338 always one-hot and the two losses are therefore equivalent. Their gradients also align when \mathbf{p}_* is
 339 one-hot, differing only by a scaling factor: $\nabla_{\mathbf{p}} \ell(\mathbf{p}, \mathbf{p}_*) = -\mathbf{p}_*$, $\nabla_{\mathbf{p}} \ell_{\text{CE}}(\mathbf{p}, \mathbf{p}_*) = -\langle \mathbf{p}, \mathbf{p}_* \rangle^{-1} \mathbf{p}_*$.
 340 Thus, the training dynamics under DP and CE losses are qualitatively identical, making the DP loss a
 341 perfect proxy for CE loss in our analysis.

342 **A.4 Stage and Order of Learning**

343 **Formal description of stages** Formally, if h_1, h_2, \dots, h_k denote the sequence of heads activated
 344 across training, then on an input sequence f_τ the model incrementally learns the functions:

$$f_\tau^\emptyset \longrightarrow f_\tau^{\{h_1\}} \longrightarrow f_\tau^{\{h_1, h_2\}} \longrightarrow \dots \longrightarrow f_\tau^{\{1, k\}},$$

345 where \emptyset is the empty set and $f_\tau^{\mathcal{N}}$ for $\mathcal{N} \subseteq [1, k]$ is a function from \mathcal{P}_{k+1} to $\Delta^{|\mathcal{R}|}$ and gives the
 346 frequency of the set $\{f_\tau(\pi) : \forall i \in \mathcal{N}, \pi_{k+1-i} = q_{k+1-i}\}$, i.e., count the frequency of output of
 347 the permutations that match q at positions in \mathcal{N} from the right.

348 **Order of learning.** A key observation concerns the order in which heads are activated. At small
 349 initialization scales, this order is determined by the relative magnitudes of the β coefficients at
 350 initialization. For example, if $\beta_{(h_1)} > \beta_{(h_2)} > \dots > \beta_{(h_k)}$, the heads are activated sequentially
 351 in the order h_1, h_2, \dots, h_k , see Fig. 4 in App.. Thus the implicit regularization induced by the scale
 352 and shape of initialization provides a natural curriculum, guiding the model to acquire the task in a
 353 stage-wise manner. For the remainder of the analysis, we assume without loss of generality that the
 354 coefficients are ordered $\beta_1 > \beta_2 > \dots > \beta_k$, so that heads are activated in order $1, 2, \dots, k$. By
 355 re-indexing the heads, the analysis for arbitrary initial orderings reduces to this canonical case.

356 **A.5 Supporting material for theoretical results**

$$\Xi = \frac{2(1+\gamma)}{(e^{\gamma_1} + k - 1)^2} \left[\frac{e^{\gamma_1}(|\mathcal{R}| - 1)}{(k-2)!|\mathcal{R}|} \right] \text{ where } \gamma_1 = (1+\gamma)\beta_1^2 \frac{e^{\alpha_1} - 1}{e^{\alpha_1} + k - 1} \quad (4)$$

357 **A.6 Subsequent Jumps and their analysis**

358 **The subsequent jumps.** Similar to the first jump, we can analyze the subsequent ones. We consider
 359 a stylized initialization, denoted \mathcal{I}_h , where $\beta_i = c$ for all $i \in [1, h-1]$, $\beta_h = \epsilon$, and $\beta_j = 0$ for
 360 all $j > h$, with c taken to be very large. Likewise, we set $\mathbf{w}^i = c_1 \mathbf{e}_i^k + c_2 \mathbf{1}$ for $i \in [1, h-1]$, and
 361 $\mathbf{w}^i = \mathbf{0}$ otherwise. Under this initialization, we study the dynamics of the h^{th} jump as the model
 362 escapes the plateau where it has learned to match $h-1$ tokens in the context. A key detail is the
 363 interplay between macroscopic parameters (the large c) and microscopic parameters (the small ϵ).
 364 In this setting, the striking feature is that the macroscopic parameters remain stationary while the
 365 microscopic ones evolve.

366 **Proposition A.2.** Consider the simplified transformer model $\theta = (\mathbf{w}^1, \mathbf{w}^2, \dots, \mathbf{w}^k, \beta)$ with k heads
 367 and initialization \mathcal{I}_h , evolving under gradient flow on the DP loss. Then:

368 (a) **Stationarity of the macroscopic variables:** The gradients of parameters in the first $h-1$
 369 heads vanish at scale $\nabla_{\mathbf{w}^i} \mathcal{L}, \nabla_{\beta_i} \mathcal{L} = O(e^{-c})$ for $i \in [1, h-1]$.
 370 (b) **Dynamics of the microscopic variables:** At $c \rightarrow \infty$, the dynamics of the remaining parameters
 371 corresponds to the those of the first jump on a task of reduced order.

372 **Stitching the jumps.** Without loss of generality, assume the initialization $\beta = (c_1\epsilon, c_2\epsilon, c_3\epsilon, \dots)$,
 373 for $c_1 > c_2 > c_3 > \dots$, with ϵ very small. Using the first-jump computations, we obtain an time
 374 T such that $\beta_1(T) > C$ for some large constant C . During this time, the gradients of the other
 375 heads remain $O(\epsilon)$, so their parameters stay close to the origin. Next, applying the subsequent-jump
 376 analysis, we can compute a time T_2 such that $\beta_2 > C$. Proceeding in this manner, we can stitch the
 377 jumps together to describe the full trajectory. This shows that, in principle, the entire evolution can
 378 be characterized by chaining together successive jumps, though we do not pursue the full analysis
 379 here, as it does not reveal qualitatively new phenomena beyond perturbation analysis.

380 **Generalizations of the simple model.** We discuss possible relaxations of the perturbed model.
 381 In particular, we highlight three illustrative generalizations. For simplification (A0), the attention
 382 window of size k provides a convenient way to compute closed-form expressions. The conservation
 383 law and the time scale can also be derived without this assumption, though in that case we lose the
 384 directional bias and the ability to obtain closed-form formulas. For simplification (A2), replacing the
 385 embeddings of the last token does not pose difficulties for the analysis. The argument still holds for
 386 the ordering $\beta_1 > \beta_2 > \beta_3 > \dots$, since the skip connection supplies the embedding of the last token
 387 for the first jump, and the head learned at jump i provides the embedding of the last token for jump
 388 $i+1$. Simplification (A3) can also be avoided by choosing a value matrix V that directly outputs the
 389 response. However, the output is not guaranteed to be a probability vector. Normalizing by the sum
 390 restores this property, making it equivalent to considering the pre-softmax scores of the responses.
 391 These generalizations indicate that the phenomena we study are robust to modest relaxations of the
 392 simplified setup, even if the algebraic convenience of the original model is lost.

393 **Experiments.** We use task of order 4 and the response vocabulary of also size 4. Overall, the results
 394 confirm our theoretical predictions: the model exhibits stage-wise plateaus followed by sharp jumps,
 395 with attention heads activating sequentially to implement recall.

396 **B Proofs of Main Results**

397 **B.1 Proof of Theorem 3.1**

398 The gradient flow of the parameters is given by

$$\begin{aligned}\dot{\beta}_h &= -\mathbb{E} \frac{\partial \ell}{\partial \beta_h}, \\ \dot{\mathbf{w}}_i^h &= -\mathbb{E} \frac{\partial \ell}{\partial \mathbf{w}_i^h}.\end{aligned}$$

399 First to show a directional bias, we will show that the trajectory always move along the manifold
 400 $\mathcal{M}_1 = \{\theta : \mathbf{w}^1 = \alpha_1 \mathbf{e}_h^1 + \delta_1 \mathbf{1}, \alpha_1, \delta_1 \in \mathbb{R} \text{ and } \beta_h, \mathbf{w}^h = 0 \text{ for } h \neq 1\}$.

401 Consider any point on the manifold \mathcal{M}_1 say $\theta = (\mathbf{w}^1, \mathbf{w}^2, \dots, \mathbf{w}^k, \beta)$ where $\mathbf{w}^1 = \alpha_1 \mathbf{e}_h^1 + \delta_1 \mathbf{1}$ and
 402 $\beta_h = 0$ for $h \neq 1$. We will show that the gradient has no component along the normal space of the
 403 manifold \mathcal{M}_1 at the point θ . Hence the trajectory will always move along the manifold \mathcal{M}_1 .

404 As the parameters satisfy the form prescribed by Lemma C.2, we can invoke the Lemma C.1 to
405 compute the gradients. The population gradients are given by

$$\mathbb{E} \frac{\partial \ell}{\partial \beta_h} = 2\beta_h \frac{e^{\alpha_h} - 1}{e^{\alpha_h} + k - 1} (1 + \gamma) \mathbb{E} \Delta_{h,h}, \quad (5)$$

$$\mathbb{E} \frac{\partial \ell}{\partial \mathbf{w}_i^h} = (1 + \gamma) \frac{\beta_h^2 ((e^{\alpha_h} - 1) \mathbb{1}\{i = h\} + 1)}{e^{\alpha_h} + k - 1} \left(\mathbb{E} \Delta_{h,i} - \frac{e^{\alpha_h} - 1}{e^{\alpha_h} + k - 1} \mathbb{E} \Delta_{h,h} \right) \quad (6)$$

406 where

$$\begin{aligned} \Delta_{h,i} &= - \left[\sum_{t=1}^{k!} \mathbf{s}_t \mathbb{1}\{r_t = r \wedge q_{k-h} = \pi_{(t,k-i)}\} - \left(\sum_{j=1}^{k!} \mathbf{s}_j \mathbb{1}\{r_j = r\} \right) \left(\sum_{t=1}^{k!} \mathbf{s}_t (\mathbb{1}\{q_{k-h} = \pi_{(t,k-i)}\}) \right) \right], \\ s &= \boldsymbol{\sigma}(\mathbf{s}'), \quad \mathbf{s}'_t = \sum_{h=1}^k \gamma_h \mathbb{1}\{q_{k-h} = \pi_{(t,k-h)}\} \\ \gamma_h &= (1 + \gamma) \beta_h^2 \frac{e^{\alpha_h} - 1}{e^{\alpha_h} + k - 1} \end{aligned}$$

407 Note that the gradients of β_h for $h \neq 1$ are zero as $\beta_h = 0$ for $h \neq 1$. Also note that the gradients of
408 \mathbf{w}^h for $h \neq 1$ are zero as $\beta_h^2 = 0$ for $h \neq 1$. The only thing that is left to show is that the gradients of
409 \mathbf{w}^1 are of the form $\frac{\partial \ell}{\partial \mathbf{w}^1} = \xi_1 \mathbf{e}_1 + \zeta_1 \mathbf{1}$ for some $\xi_1, \zeta_1 \in \mathbb{R}$.

410 Note that $\mathbf{s}'_t = \gamma_1 \mathbb{1}\{q_{k-1} = \pi_{(t,k-1)}\}$ as $\gamma_h = 0$ for $h \neq 1$ and the softmax score is given by

$$\mathbf{s}_t = \frac{e^{\gamma_1 \mathbb{1}\{q_{k-1} = \pi_{(t,k-1)}\}}}{\sum_{j=1}^{k!} e^{\gamma_1 \mathbb{1}\{q_{k-1} = \pi_{(j,k-1)}\}}} = \frac{(e^{\gamma_1} - 1) \mathbb{1}\{q_{k-1} = \pi_{(t,k-1)}\} + 1}{e^{\gamma_1} + k - 1} \frac{1}{(k-1)!}.$$

411 From Lemma C.3 we have

$$\begin{aligned} \mathbb{E} \Delta_{1,i} &= \frac{1}{(e^{\gamma_1} + k - 1)^2} \left[\frac{e^{\gamma_1} (|\mathcal{R}| - 1)}{(k-1)! |\mathcal{R}|} \right], \quad \text{for } i \neq 1. \\ \mathbb{E} \Delta_{1,1} &= -(k-1) \mathbb{E} \Delta_{1,i} = -\frac{1}{(e^{\gamma_1} + k - 1)^2} \left[\frac{e^{\gamma_1} (|\mathcal{R}| - 1)}{(k-2)! |\mathcal{R}|} \right]. \end{aligned}$$

412 So the gradient of \mathbf{w}_i^1 given by $\frac{\partial \ell}{\partial \mathbf{w}_i^1}$ is independent of i for $i \neq 1$ since $\mathbb{E} \Delta_{1,i}$ is independent of i .

413 Hence the gradient of \mathbf{w}^1 is of the form $\frac{\partial \ell}{\partial \mathbf{w}^1} = \xi_1 \mathbf{e}_1 + \zeta_1 \mathbf{1}$ for some $\xi_1, \zeta_1 \in \mathbb{R}$. This proves the
414 directional bias of the trajectory.

415 For the next signal propagation part of the result, we will show that there exists note that $\mathbb{E} \Delta_{1,1} < 0$
416 for all $\gamma_1 > 0$ and $\mathbb{E} \Delta_{1,i} > 0$ for all $\gamma_1 > 0$ and $i \neq 1$. Using these expressions, the population
417 gradient of \mathbf{w}_1^1 is given by

$$\begin{aligned} \mathbb{E} \frac{\partial \ell}{\partial \mathbf{w}_1^1} &= (1 + \gamma) \frac{\beta_1^2 e^{\alpha_1}}{e^{\alpha_1} + k - 1} \left(\mathbb{E} \Delta_{1,1} - \frac{e^{\alpha_1} - 1}{e^{\alpha_1} + k - 1} \mathbb{E} \Delta_{1,1} \right) \\ &= (1 + \gamma) \frac{\beta_1^2 e^{\alpha_1}}{e^{\alpha_1} + k - 1} \left(\frac{k-1}{e^{\alpha_1} + k - 1} \mathbb{E} \Delta_{1,1} \right) < 0 \end{aligned}$$

418 Similarly the population gradient of \mathbf{w}_i^1 for $i \neq 1$ is given by

$$\begin{aligned} \mathbb{E} \frac{\partial \ell}{\partial \mathbf{w}_i^1} &= (1 + \gamma) \frac{\beta_1^2}{e^{\alpha_1} + k - 1} \left(\mathbb{E} \Delta_{1,i} - \frac{e^{\alpha_1} - 1}{e^{\alpha_1} + k - 1} \mathbb{E} \Delta_{1,1} \right), \\ &= (1 + \gamma) \frac{\beta_1^2}{e^{\alpha_1} + k - 1} \left(-\frac{\mathbb{E} \Delta_{1,1}}{k-1} - \frac{e^{\alpha_1} - 1}{e^{\alpha_1} + k - 1} \mathbb{E} \Delta_{1,1} \right), \\ &> 0 \end{aligned}$$

419 The dynamics of gradient descent is given by

$$\begin{aligned}\dot{\mathbf{w}}_1 &= -\mathbb{E} \frac{\partial \ell}{\partial \mathbf{w}_1} = -(1+\gamma) \frac{\beta_1^2 e^{\alpha_1}}{e^{\alpha_1} + k - 1} \left(\frac{k}{e^{\alpha_1} + k - 1} \mathbb{E} \Delta_{1,1} \right) > 0, \\ \dot{\mathbf{w}}_i &= -\mathbb{E} \frac{\partial \ell}{\partial \mathbf{w}_i} = (1+\gamma) \frac{\beta_1^2}{e^{\alpha_1} + k - 1} \left(-\frac{\mathbb{E} \Delta_{1,1}}{k-1} - \frac{e^{\alpha_1} - 1}{e^{\alpha_1} + k - 1} \mathbb{E} \Delta_{1,1} \right) < 0, \quad i \neq 1 \\ \dot{\beta}_1 &= -\mathbb{E} \frac{\partial \ell}{\partial \beta_1} = -2\beta_1 \frac{e^{\alpha_1} - 1}{e^{\alpha_1} + k - 1} (1+\gamma) \mathbb{E} \Delta_{1,1} > 0\end{aligned}$$

420 The complete dynamics of the system is given by $\dot{\alpha}_1, \dot{\beta}_1$ and they can be written as

$$\begin{aligned}\dot{\alpha}_1 &= \dot{\mathbf{w}}_1 - \dot{\mathbf{w}}_2 = (1+\gamma) \frac{\beta_1^2}{e^{\alpha_1} + k - 1} \left(\frac{(k)e^{\alpha_1}}{e^{\alpha_1} + k - 1} \mathbb{E} \Delta_{1,1} + \frac{\mathbb{E} \Delta_{1,1}}{k-1} + \frac{e^{\alpha_1} - 1}{e^{\alpha_1} + k - 1} \mathbb{E} \Delta_{1,1} \right) < 0, \\ \dot{\beta}_1 &= -2\beta_1 \frac{e^{\alpha_1} - 1}{e^{\alpha_1} + k - 1} (1+\gamma) \mathbb{E} \Delta_{1,1} > 0\end{aligned}$$

421 The final system of ODE is given by ,

$$\begin{aligned}\dot{\alpha}_1 &= \frac{\beta_1^2 e^{\alpha_1}}{e^{\alpha_1} + k - 1}^2 \frac{k^2}{k-1} - \mathbb{E}(1+\gamma) \Delta_{1,1}, \\ \dot{\beta}_1 &= 2\beta_1 \frac{e^{\alpha_1} - 1}{e^{\alpha_1} + k - 1} - \mathbb{E}(1+\gamma) \Delta_{1,1}\end{aligned}$$

422 Lets denote $\Xi = -2(1+\gamma)\mathbb{E} \Delta_{1,1}$ which is positive and given by

$$\Xi = \frac{2(1+\gamma)}{(e^{\gamma_1} + k - 1)^2} \left[\frac{e^{\gamma_1}(|\mathcal{R}| - 1)}{(k-2)!|\mathcal{R}|} \right] \text{ where } \gamma_1 = (1+\gamma)\beta_1^2 \frac{e^{\alpha_1} - 1}{e^{\alpha_1} + k - 1}$$

423 Using this the system of ODE can be written as

$$\begin{aligned}\dot{\alpha}_1 &= \frac{\beta_1^2 e^{\alpha_1}}{(e^{\alpha_1} + k - 1)^2} \frac{k^2}{k-1} \Xi, \\ \dot{\beta}_1 &= 2\beta_1 \frac{e^{\alpha_1} - 1}{e^{\alpha_1} + k - 1} \Xi\end{aligned}$$

424 Note that

$$\frac{\dot{\beta}_1^2}{4} = \beta_1^2 \frac{e^{\alpha_1} - 1}{e^{\alpha_1} + k - 1} \Xi$$

425

$$f(\dot{\alpha}_1) = f'(\alpha_1) \dot{\alpha}_1 = f'(\alpha_1) \frac{\beta_1^2 e^{\alpha_1}}{(e^{\alpha_1} + k - 1)^2} \frac{k^2}{k-1} \Xi$$

426 If we choose $f(\alpha_1)$ such that

$$\begin{aligned}f'(\alpha_1) \frac{\beta_1^2 e^{\alpha_1}}{(e^{\alpha_1} + k - 1)^2} \frac{k^2}{k-1} \Xi &= \beta_1^2 \frac{e^{\alpha_1} - 1}{e^{\alpha_1} + k - 1} \Xi, \\ \implies f'(\alpha_1) &= \frac{k-1}{k^2} \frac{(e^{\alpha_1} - 1)(e^{\alpha_1} - 1 + k)}{e^{\alpha_1}} \\ &= \frac{k-1}{k^2} (e^{\alpha_1} - 2 + e^{-\alpha_1} - ke^{-\alpha_1} + k) \\ \implies f(\alpha_1) &= \frac{k-1}{k^2} (e^{\alpha_1} - 2\alpha_1 - e^{-\alpha_1} + ke^{-\alpha_1} + k\alpha_1), \\ f(\alpha_1) &= 2\frac{k-1}{k^2} (\sinh(\alpha_1) - \alpha_1) + \frac{k-1}{k} [e^{-\alpha_1} + \alpha_1 - 1]\end{aligned}$$

427 Now $f(\alpha_1) - \beta_1^2/4$ is conserved along the trajectory. As $d(f(\alpha_1) - \beta_1^2/4) = 0$.

428 This completes the proof of the theorem.

429 **B.2 Proof of Theorem A.2**

430 The gradient flow is given by The population gradients are given by

$$\mathbb{E} \frac{\partial \ell}{\partial \beta_h} = 2\beta_h \frac{e^{\alpha_h} - 1}{e^{\alpha_h} + k - 1} (1 + \gamma) \mathbb{E} \Delta_{h,h}, \quad (7)$$

$$\mathbb{E} \frac{\partial \ell}{\partial \mathbf{w}_i^h} = (1 + \gamma) \frac{\beta_h^2 ((e^{\alpha_h} - 1) \mathbb{1}\{i = h\} + 1)}{e^{\alpha_h} + k - 1} \left(\mathbb{E} \Delta_{h,i} - \frac{e^{\alpha_h} - 1}{e^{\alpha_h} + k - 1} \mathbb{E} \Delta_{h,h} \right) \quad (8)$$

431 where

$$\begin{aligned} \Delta_{h,i} &= - \left[\sum_{t=1}^{k!} \mathbf{s}_t \mathbb{1}\{r_t = r \wedge q_{k-h} = \pi_{(t,k-i)}\} - \left(\sum_{j=1}^{k!} \mathbf{s}_j \mathbb{1}\{r_j = r\} \right) \left(\sum_{t=1}^{k!} \mathbf{s}_t (\mathbb{1}\{q_{k-h} = \pi_{(t,k-i)}\}) \right) \right], \\ s &= \sigma(\mathbf{s}'), \quad \mathbf{s}'_t = \sum_{h=1}^k \gamma_h \mathbb{1}\{q_{k-h} = \pi_{(t,k-h)}\} \\ \gamma_h &= (1 + \gamma) \beta_h^2 \frac{e^{\alpha_h} - 1}{e^{\alpha_h} + k - 1} \end{aligned}$$

432 Without loss of generality, assume that $\gamma_i = c$ for $i \in [1, h-1]$. Now split the set of permutations
433 into two partitions \mathcal{P}_S and \mathcal{P}_S^c where for query q , \mathcal{P}_S is the set that matches the last $h-1$ tokens
434 and others do not. Now $\mathbf{s}_t = e^{-c}$ for $t \in \mathcal{P}_S^c$. Now $\Delta_{i,j}$ for $i \in [1, h-1]$ and $j \neq i$, it can be seen that
435 $\mathbf{s}_t (\mathbb{1}\{q_{k-i} = \pi_{(t,k-j)}\}) = e^{-c}$ for any t , hence $\mathbb{E} \Delta_{i,j} = e^{-c}$. The cases left are $\mathbb{E} \Delta_{i,i}$, but it is also
436 of e^{-c} as the $\Delta_{i,:}$'s sum to 0.

437 Now the case of $i = h$, now for $t \in \mathcal{P}_S$

$$\begin{aligned} s_t &= \frac{\exp\{c\} \exp\{\gamma_h \mathbb{1}\{q_{k-h} = \pi_{(t,k-h)}\}\}}{\sum_{\pi_t \in \mathcal{P}_S} \exp\{c\} \exp\{\gamma_h \mathbb{1}\{q_{k-h} = \pi_{(t,k-h)}\}\} + O(1)}, \\ &= \frac{\exp\{\gamma_h \mathbb{1}\{q_{k-h} = \pi_{(t,k-h)}\}\}}{\sum_{\pi_t \in \mathcal{P}_S} \exp\{\gamma_h \mathbb{1}\{q_{k-h} = \pi_{(t,k-h)}\}\}} + O(e^{-c}) \end{aligned}$$

438 This expression is exactly equivalent to the first jump however now restricted on the set \mathcal{P}_S of reduced
439 order.

440 **C Computations of the derivatives of the simplified transformer model**

441 The forward pass of the simplified transformer model on a single input sequence is given by, let r be
442 the response of the query.

$$\mathbf{R}_i^h = \sum_{j=i-k}^{i-1} \sigma(\mathbf{A}^h)_{ij} e_{x_j}, \quad (9a)$$

$$\tilde{\mathbf{s}}_t = \sum_{h=1}^k \beta_h^2 \langle e_{x_{l-h}}, \tilde{\mathbf{I}}_k \mathbf{R}_t^h \rangle, \quad (9b)$$

$$\mathbf{s} = \sigma(\tilde{\mathbf{s}}_{\mathcal{R}}) \quad (9c)$$

$$\mathbf{p} = \sum_{t:x_t \in \mathcal{R}} \mathbf{s}_t e_{x_t} \quad (9d)$$

$$\ell = 1 - \langle \mathbf{p}, e_r \rangle \quad (9e)$$

443 For the convenience of the analysis, we will drop \mathcal{R} in the subscript of $\tilde{\mathbf{s}}$ and now $\tilde{\mathbf{s}} \in \mathbb{R}^{k!}$ where $\tilde{\mathbf{s}}_t$
444 denotes the score of the response corresponding to the t^{th} permutation in the sequence.

445 **Derivatives wrt to the $\tilde{\mathbf{s}}$.** The derivatives of the loss with respect to the predicted scores can be
446 computed using the chain rule:

$$\frac{\partial \ell}{\partial \tilde{\mathbf{s}}} = \frac{\partial \ell}{\partial \mathbf{p}} \frac{\partial \mathbf{p}}{\partial \mathbf{s}} \frac{\partial \mathbf{s}}{\partial \tilde{\mathbf{s}}} = -e_r^\top \mathbf{X}_{\mathcal{R}}^\top (\text{diag}(\mathbf{s}) - \mathbf{s} \mathbf{s}^\top).$$

447 The co-ordinate wise derivative is

$$\frac{\partial \ell}{\partial \tilde{\mathbf{s}}_t} = -\mathbf{s}_t \left(\mathbb{1}\{r_t = r\} - \sum_{j=1}^{k!} \mathbf{s}_j \mathbb{1}\{r_j = r\} \right) = \ell'_t.$$

448 where r_t is the response corresponding to the t^{th} permutation in the sequence. Using the property of
449 the softmax we have $\ell(\tilde{\mathbf{s}} + c\mathbf{1}) = \ell(\tilde{\mathbf{s}})$ as the softmax is invariant when even co-ordinate is shifted by
450 a constant. Now taking the derivative with c at $c = 0$ we get

$$\sum_{t=1}^{k!} \ell'_t = 0 \quad (10)$$

451 **Derivative of $\tilde{\mathbf{s}}$ wrt to β and \mathbf{w}^h 's** The derivative of $\tilde{\mathbf{s}}$ with respect to β can be computed as
452 follows:

$$\frac{\partial \tilde{\mathbf{s}}_t}{\partial \beta_h} = 2\beta_h \left\langle e_{x_{l-h}}, \tilde{\mathbf{I}}_k \mathbf{R}_t^h \right\rangle$$

453 The derivative of $\tilde{\mathbf{s}}$ with respect to \mathbf{w}_i^h can be computed as follows:

$$\frac{\partial \tilde{\mathbf{s}}_t}{\partial \mathbf{w}_i^h} = \beta_h^2 \left\langle e_{x_{l-h}}, \tilde{\mathbf{I}}_k \frac{\partial \mathbf{R}_t^h}{\partial \mathbf{w}_i^h} \right\rangle$$

454 Using Lemma D.2 we have

$$\begin{aligned} \frac{\partial \tilde{\mathbf{s}}_t}{\partial \mathbf{w}_i^h} &= \beta_h^2 \left\langle e_{x_{l-h}}, \tilde{\mathbf{I}}_k \frac{e^{\mathbf{w}_i^h}}{\sum_{j=1}^k e^{\mathbf{w}_j^h}} (e_{\pi_{(t,k-i)}} - \mathbf{R}_t^h) \right\rangle \\ &= \beta_h^2 \frac{e^{\mathbf{w}_i^h}}{\sum_{j=1}^k e^{\mathbf{w}_j^h}} \left(\left\langle e_{x_{l-h}}, \tilde{\mathbf{I}}_k e_{\pi_{(t,k-i)}} \right\rangle - \left\langle e_{x_{l-h}}, \tilde{\mathbf{I}}_k \mathbf{R}_t^h \right\rangle \right) \end{aligned}$$

455 Note that $x_{l-h} = q_{k-h}$ and $\left\langle e_{x_{l-h}}, \tilde{\mathbf{I}}_k e_{\pi_{(t,k-i)}} \right\rangle = \mathbb{1}\{q_{k-h} = \pi_{(t,k-i)}\} - \gamma \mathbb{1}\{q_{k-h} \neq \pi_{(t,k-i)}\} \mathbb{1}\{q_{k-h} = \pi_{(t,k-i)}\} - \gamma$. Using this computation, we have,

$$\frac{\partial \tilde{\mathbf{s}}_t}{\partial \mathbf{w}_i^h} = \frac{\beta_h^2 e^{\mathbf{w}_i^h}}{\sum_{j=1}^k e^{\mathbf{w}_j^h}} \left((1 + \gamma) \mathbb{1}\{q_{k-h} = \pi_{(t,k-i)}\} - \gamma - \left\langle e_{x_{l-h}}, \tilde{\mathbf{I}}_k \mathbf{R}_t^h \right\rangle \right)$$

457 Computing the derivative of the loss with respect to β and \mathbf{w}_i^h we have

$$\begin{aligned} \frac{\partial \ell}{\partial \beta_h} &= \sum_{t=1}^{k!} \ell'_t 2\beta_h \left\langle e_{x_{l-h}}, \tilde{\mathbf{I}}_k \mathbf{R}_t^h \right\rangle = 2\beta_h \sum_{t=1}^{k!} \ell'_t \left\langle e_{x_{l-h}}, \tilde{\mathbf{I}}_k \mathbf{R}_t^h \right\rangle \\ \frac{\partial \ell}{\partial \mathbf{w}_i^h} &= \sum_{t=1}^{k!} \ell'_t \frac{\beta_h^2 e^{\mathbf{w}_i^h}}{\sum_{j=1}^k e^{\mathbf{w}_j^h}} \left((1 + \gamma) \mathbb{1}\{q_{k-h} = \pi_{(t,k-i)}\} - \gamma - \left\langle e_{x_{l-h}}, \tilde{\mathbf{I}}_k \mathbf{R}_t^h \right\rangle \right), \\ &= \frac{\beta_h^2 e^{\mathbf{w}_i^h}}{\sum_{j=1}^k e^{\mathbf{w}_j^h}} \sum_{t=1}^{k!} \ell'_t \left((1 + \gamma) \mathbb{1}\{q_{k-h} = \pi_{(t,k-i)}\} - \left\langle e_{x_{l-h}}, \tilde{\mathbf{I}}_k \mathbf{R}_t^h \right\rangle \right), \end{aligned}$$

458 Now collecting the final expressions we have the following lemma.

459 **Lemma C.1.** *The derivatives of the loss ℓ with respect to the parameters β and \mathbf{w}^h 's are given by*

$$\begin{aligned} \frac{\partial \ell}{\partial \beta_h} &= 2\beta_h \sum_{t=1}^{k!} \ell'_t \left\langle e_{x_{l-h}}, \tilde{\mathbf{I}}_k \mathbf{R}_t^h \right\rangle \\ \frac{\partial \ell}{\partial \mathbf{w}_i^h} &= \frac{\beta_h^2 e^{\mathbf{w}_i^h}}{\sum_{j=1}^k e^{\mathbf{w}_j^h}} \sum_{t=1}^{k!} \ell'_t \left((1 + \gamma) \mathbb{1}\{q_{k-h} = \pi_{(t,k-i)}\} - \left\langle e_{x_{l-h}}, \tilde{\mathbf{I}}_k \mathbf{R}_t^h \right\rangle \right), \end{aligned}$$

460 where $\ell'_t = -\mathbf{s}_t \left(\mathbb{1}\{r_t = r\} - \sum_{j=1}^{k!} \mathbf{s}_j \mathbb{1}\{r_j = r\} \right)$.

461 The proof of the lemma is given above.

462 Now we will use the above lemma to compute the gradients at a particular parameter configuration,
463 we choose a general parameter configuration so that we can invoke this lemma whenever gradient
464 computations are needed.

465 **Lemma C.2.** *Consider a parameter configuration \mathcal{I}_G defined such that for all h and i ,*

$$\mathbf{w}^h = \alpha_h \mathbf{e}_h^k + \delta_h \mathbf{1}$$

466 β_h is used as is. Then the gradients at this parameter configuration are given by

$$\frac{\partial \ell}{\partial \beta_h} = 2\beta_h \frac{e^{\alpha_h} - 1}{e^{\alpha_h} + k - 1} (1 + \gamma) \Delta_{h,h}, \quad (11)$$

$$\frac{\partial \ell}{\partial \mathbf{w}_i^h} = (1 + \gamma) \frac{\beta_h^2 e^{\alpha_h + \delta_h}}{e^{\alpha_h} + k - 1} \left(\Delta_{h,i} - \frac{e^{\alpha_h} - 1}{e^{\alpha_h} + k - 1} \Delta_{h,h} \right) \quad (12)$$

467 where

$$\Delta_{h,i} = - \left[\sum_{t=1}^{k!} \mathbf{s}_t \mathbb{1}\{r_t = r \wedge q_{k-h} = \pi_{(t,k-i)}\} - \left(\sum_{j=1}^{k!} \mathbf{s}_j \mathbb{1}\{r_j = r\} \right) \left(\sum_{t=1}^{k!} \mathbf{s}_t (\mathbb{1}\{q_{k-h} = \pi_{(t,k-i)}\}) \right) \right]$$

468 where $s = \sigma(\mathbf{s}')$ and $\mathbf{s}_t' = \sum_{h=1}^k \gamma_h \mathbb{1}\{q_{k-h} = \pi_{(t,k-h)}\}$ with $\gamma_h = (1 + \gamma) \beta_h^2 \frac{e^{\alpha_h} - 1}{e^{\alpha_h} + k - 1}$.

469 *Proof.* First let us compute the forward pass

$$\begin{aligned} \mathbf{R}_t^h &= \sum_{i=1}^k \sigma(\mathbf{A}^h)_{t,t-i} e_{\pi_{(t,k-i)}} = \sum_{i=1}^k \frac{e^{\mathbf{w}_i^h}}{\sum_{j=1}^k e^{\mathbf{w}_j^h}} e_{\pi_{(t,k-i)}}, \\ &= \frac{e^{\alpha_h + \delta_h}}{(e^{\alpha_h} + k - 1) e^{\delta_h}} e_{\pi_{(t,k-h)}} + \sum_{i \neq h} \frac{e^{\delta_h}}{(e^{\alpha_h} + k - 1) e^{\delta_h}} e_{\pi_{(t,k-i)}}, \\ &= \frac{e^{\alpha_h} - 1}{e^{\alpha_h} + k - 1} e_{\pi_{(t,k-h)}} + \frac{1}{e^{\alpha_h} + k - 1} \mu \end{aligned}$$

470 Note that $\mu = \sum_{i=1}^k e_{\pi_{(t,k-i)}}$ is the same for all t . Now the presoftmax score is given by

$$\begin{aligned} \tilde{\mathbf{s}}_t &= \sum_{h=1}^k \beta_h^2 \left\langle e_{x_{t-h}}, \tilde{\mathbf{I}}_k \mathbf{R}_t^h \right\rangle, \\ &= \sum_{h=1}^k \beta_h^2 \left(\frac{e^{\alpha_h} - 1}{e^{\alpha_h} + k - 1} (1 + \gamma) \mathbb{1}\{q_{k-h} = \pi_{(t,k-h)}\} - \gamma - \frac{1}{e^{\alpha_h} + k - 1} (1 + \gamma) \right), \\ &= (1 + \gamma) \sum_{h=1}^k \beta_h^2 \frac{e^{\alpha_h} - 1}{e^{\alpha_h} + k - 1} \mathbb{1}\{q_{k-h} = \pi_{(t,k-h)}\} - (1 + \gamma) \sum_{h=1}^k \frac{\beta_h^2}{e^{\alpha_h} + k - 1} - \gamma \sum_{h=1}^k \beta_h^2. \end{aligned}$$

471 Define

$$\gamma_h = (1 + \gamma) \beta_h^2 \frac{e^{\alpha_h} - 1}{e^{\alpha_h} + k - 1}. \quad (13)$$

472 Denote

$$\mathbf{s}_t' = \sum_{h=1}^k \gamma_h \mathbb{1}\{q_{k-h} = \pi_{(t,k-h)}\}.$$

473 Note that $\tilde{\mathbf{s}}_t = \mathbf{s}'_t + c$ where c is a constant independent of t . Using the property of the softmax we
474 have $\mathbf{s} = \ell(\mathbf{s}')$. Using the lemma C.1 we have

$$\begin{aligned}
\frac{\partial \ell}{\partial \beta_h} &= 2\beta_h \sum_{t=1}^{k!} \ell'_t \left\langle e_{x_{l-h}}, \tilde{\mathbf{I}}_k \mathbf{R}_t^h \right\rangle, \\
&= 2\beta_h \sum_{t=1}^{k!} \ell'_t \left(\frac{e^{\alpha_h} - 1}{e^{\alpha_h} + k - 1} (1 + \gamma) \mathbb{1}\{q_{k-h} = \pi_{(t,k-h)}\} - \gamma - \frac{1}{e^{\alpha_h} + k - 1} (1 + \gamma) \right), \\
&= 2\beta_h \frac{e^{\alpha_h} - 1}{e^{\alpha_h} + k - 1} (1 + \gamma) \sum_{t=1}^{k!} \ell'_t \mathbb{1}\{q_{k-h} = \pi_{(t,k-h)}\} - 2\beta_h \left(\gamma + \frac{1}{e^{\alpha_h} + k - 1} (1 + \gamma) \right) \sum_{t=1}^{k!} \ell'_t, \\
&= 2\beta_h \frac{e^{\alpha_h} - 1}{e^{\alpha_h} + k - 1} (1 + \gamma) \sum_{t=1}^{k!} \ell'_t \mathbb{1}\{q_{k-h} = \pi_{(t,k-h)}\},
\end{aligned}$$

475 Now the derivative with respect to \mathbf{w}_i^h is given by

$$\begin{aligned}
\frac{\partial \ell}{\partial \mathbf{w}_i^h} &= \frac{\beta_h^2 e^{\mathbf{w}_i^h}}{\sum_{j=1}^k e^{\mathbf{w}_j^h}} \sum_{t=1}^{k!} \ell'_t \left((1 + \gamma) \mathbb{1}\{q_{k-h} = \pi_{(t,k-i)}\} - \left\langle e_{x_{l-h}}, \tilde{\mathbf{I}}_k \mathbf{R}_t^h \right\rangle \right), \\
&= \frac{\beta_h^2 e^{\alpha_h + \delta_h}}{e^{\alpha_h} + k - 1} \sum_{t=1}^{k!} \ell'_t \left((1 + \gamma) \mathbb{1}\{q_{k-h} = \pi_{(t,k-i)}\} - \left\langle e_{x_{l-h}}, \tilde{\mathbf{I}}_k \mathbf{R}_t^h \right\rangle \right), \\
&= \frac{\beta_h^2 e^{\alpha_h + \delta_h}}{e^{\alpha_h} + k - 1} \sum_{t=1}^{k!} \ell'_t \left((1 + \gamma) \mathbb{1}\{q_{k-h} = \pi_{(t,k-i)}\} - \frac{e^{\alpha_h} - 1}{e^{\alpha_h} + k - 1} (1 + \gamma) \ell'_t \mathbb{1}\{q_{k-h} = \pi_{(t,k-h)}\} \right), \\
&= (1 + \gamma) \frac{\beta_h^2 e^{\alpha_h + \delta_h}}{e^{\alpha_h} + k - 1} \sum_{t=1}^{k!} \ell'_t \left(\mathbb{1}\{q_{k-h} = \pi_{(t,k-i)}\} - \frac{e^{\alpha_h} - 1}{e^{\alpha_h} + k - 1} \mathbb{1}\{q_{k-h} = \pi_{(t,k-h)}\} \right),
\end{aligned}$$

476 We introduce a notation where

$$\Delta_{h,i} = \sum_{t=1}^{k!} \ell'_t (\mathbb{1}\{q_{k-h} = \pi_{(t,k-i)}\})$$

477 Using this notation, the gradients can be written as

$$\begin{aligned}
\frac{\partial \ell}{\partial \beta_h} &= 2\beta_h \frac{e^{\alpha_h} - 1}{e^{\alpha_h} + k - 1} (1 + \gamma) \Delta_{h,h}, \\
\frac{\partial \ell}{\partial \mathbf{w}_i^h} &= (1 + \gamma) \frac{\beta_h^2 e^{\alpha_h + \delta_h}}{e^{\alpha_h} + k - 1} \left(\Delta_{h,i} - \frac{e^{\alpha_h} - 1}{e^{\alpha_h} + k - 1} \Delta_{h,h} \right),
\end{aligned}$$

478 where $\Delta_{h,i} = \sum_{t=1}^{k!} \ell'_t (\mathbb{1}\{q_{k-h} = \pi_{(t,k-i)}\})$. Substituting the expression of ℓ'_t we have

$$\begin{aligned}
\Delta_{h,i} &= \sum_{t=1}^{k!} -\mathbf{s}_t \left(\mathbb{1}\{r_t = r\} - \sum_{j=1}^{k!} \mathbf{s}_j \mathbb{1}\{r_j = r\} \right) (\mathbb{1}\{q_{k-h} = \pi_{(t,k-i)}\}), \\
&= - \left[\sum_{t=1}^{k!} \mathbf{s}_t \mathbb{1}\{r_t = r \wedge q_{k-h} = \pi_{(t,k-i)}\} - \left(\sum_{j=1}^{k!} \mathbf{s}_j \mathbb{1}\{r_j = r\} \right) \left(\sum_{t=1}^{k!} \mathbf{s}_t (\mathbb{1}\{q_{k-h} = \pi_{(t,k-i)}\}) \right) \right],
\end{aligned}$$

$$\Delta_{h,i} = - \left[\sum_{t=1}^{k!} \mathbf{s}_t \mathbb{1}\{r_t = r \wedge q_{k-h} = \pi_{(t,k-i)}\} - \left(\sum_{j=1}^{k!} \mathbf{s}_j \mathbb{1}\{r_j = r\} \right) \left(\sum_{t=1}^{k!} \mathbf{s}_t (\mathbb{1}\{q_{k-h} = \pi_{(t,k-i)}\}) \right) \right]. \quad (14)$$

479 where $s = \sigma(\mathbf{s}')$. This completes the proof of the lemma.

480 \square

481 **Lemma C.3.** *For the parameter configuration $\theta = (\mathbf{w}^1, \mathbf{w}^2, \dots, \mathbf{w}^k, \beta)$ where $\mathbf{w}^1 = \alpha_1 \mathbf{e}_h^1 + \delta_1 \mathbf{1}$ and $\beta_h = 0$ for $h \neq 1$. The following quantities are*

$$\begin{aligned} \mathbb{E}\Delta_{1,i} &= \frac{1}{(e^{\gamma_1} + k - 1)^2} \left[\frac{e^{\gamma_1} (|\mathcal{R}| - 1)}{(k - 1)! |\mathcal{R}|} \right], \quad \text{for } i \neq 1. \\ \mathbb{E}\Delta_{1,1} &= -(k - 1) \mathbb{E}\Delta_{1,i} = -\frac{1}{(e^{\gamma_1} + k - 1)^2} \left[\frac{e^{\gamma_1} (|\mathcal{R}| - 1)}{(k - 2)! |\mathcal{R}|} \right]. \end{aligned}$$

483 where $\gamma_1 = (1 + \gamma) \beta_1^2 \frac{e^{\alpha_1} - 1}{e^{\alpha_1} + k - 1}$.

484 *Proof.* Recall that $\mathbf{s}_t' = \gamma_1 \mathbb{1}\{q_{k-1} = \pi_{(t,k-1)}\}$ as $\gamma_h = 0$ for $h \neq 1$ and the softmax score is given by

$$\mathbf{s}_t = \frac{e^{\gamma_1} \mathbb{1}\{q_{k-1} = \pi_{(t,k-1)}\}}{\sum_{j=1}^{k!} e^{\gamma_1} \mathbb{1}\{q_{k-1} = \pi_{(j,k-1)}\}} = \frac{(e^{\gamma_1} - 1) \mathbb{1}\{q_{k-1} = \pi_{(t,k-1)}\} + 1}{e^{\gamma_1} + k - 1} \frac{1}{(k - 1)!}.$$

485 First lets compute $\mathbb{E}\Delta_{1,i}$ for $i \neq 1$, Note that

$$\begin{aligned} \sum_{t=1}^{k!} \mathbf{s}_t (\mathbb{1}\{q_{k-1} = \pi_{(t,k-i)}\}) &= \sum_{t=1}^{k!} \frac{(e^{\gamma_1} - 1) \mathbb{1}\{q_{k-1} = \pi_{(t,k-i)}\} + 1}{e^{\gamma_1} + k - 1} \frac{1}{(k - 1)!} (\mathbb{1}\{q_{k-1} = \pi_{(t,k-i)}\}), \\ &= \frac{1}{e^{\gamma_1} + k - 1}. \end{aligned}$$

486 For $i = 1$, we have,

$$\begin{aligned} \sum_{t=1}^{k!} \mathbf{s}_t (\mathbb{1}\{q_{k-1} = \pi_{(t,k-i)}\}) &= \sum_{t=1}^{k!} \frac{(e^{\gamma_1} - 1) \mathbb{1}\{q_{k-1} = \pi_{(t,k-i)}\} + 1}{e^{\gamma_1} + k - 1} \frac{1}{(k - 1)!} (\mathbb{1}\{q_{k-1} = \pi_{(t,k-i)}\}), \\ &= \frac{e^{\gamma_1}}{e^{\gamma_1} + k - 1}. \end{aligned}$$

487 Now we can compute $\mathbb{E}\Delta_{1,i}$ for $i \neq 1$ as follows:

$$\begin{aligned} \mathbb{E}\Delta_{1,i} &= -\mathbb{E} \left[\sum_{t=1}^{k!} \mathbf{s}_t \mathbb{1}\{r_t = r \wedge q_{k-1} = \pi_{(t,k-i)}\} - \left(\sum_{j=1}^{k!} \mathbf{s}_j \mathbb{1}\{r_j = r\} \right) \left(\sum_{t=1}^{k!} \mathbf{s}_t (\mathbb{1}\{q_{k-1} = \pi_{(t,k-i)}\}) \right) \right], \\ &= -\mathbb{E} \left[\sum_{t=1}^{k!} \mathbf{s}_t \mathbb{1}\{r_t = r \wedge q_{k-1} = \pi_{(t,k-i)}\} \right] + \mathbb{E} \left[\left(\sum_{j=1}^{k!} \mathbf{s}_j \mathbb{1}\{r_j = r\} \right) \frac{1}{e^{\gamma_1} + k - 1} \right], \end{aligned}$$

488 For $i \neq 1$,

$$\begin{aligned} \mathbb{E} \left[\sum_{t=1}^{k!} \mathbf{s}_t \mathbb{1}\{r_t = r \wedge q_{k-1} = \pi_{(t,k-i)}\} \right] &= \frac{1}{e^{\gamma_1} + k - 1} \frac{1}{(k - 1)!} \mathbb{E} \left[\sum_{t=1}^{k!} \mathbb{1}\{r_t = r \wedge q_{k-1} = \pi_{(t,k-i)}\} \right], \\ &= \frac{1}{e^{\gamma_1} + k - 1} \frac{1}{(k - 1)!} \sum_{t=1}^{k!} \mathbb{P}(r_t = r \wedge q_{k-1} = \pi_{(t,k-i)}), \end{aligned}$$

489 Note that for $i \neq 1$, $\mathbb{P}(r_t = r \wedge q_{k-1} = \pi_{(t,k-i)}) = \mathbb{P}(r_t = r)\mathbb{P}(q_{k-1} = \pi_{(t,k-i)})$ due to the
490 independence as q is not same as π_t . $\mathbb{P}(q_{k-1} = \pi_{(t,k-i)}) = \frac{1}{k}$ as q_{k-1} is uniformly distributed over
491 $[k]$. $\mathbb{P}(r_t = r) = \frac{1}{|\mathcal{R}|}$. So,

$$\mathbb{E} \left[\sum_{t=1}^{k!} \mathbf{s}_t \mathbb{1}\{r_t = r \wedge q_{k-1} = \pi_{(t,k-i)}\} \right] = \frac{1}{e^{\gamma_1} + k - 1} \frac{1}{(k-1)!} \sum_{t=1}^{k!} \frac{1}{k|\mathcal{R}|} = \frac{1}{e^{\gamma_1} + k - 1} \frac{1}{|\mathcal{R}|}.$$

492 Now for $i = 1$,

$$E \left[\sum_{t=1}^{k!} \mathbf{s}_t \mathbb{1}\{r_t = r \wedge q_{k-1} = \pi_{(t,k-1)}\} \right] = \frac{e^{\gamma_1}}{e^{\gamma_1} + k - 1} \frac{1}{(k-1)!} \mathbb{E} \left[\sum_{t=1}^{k!} \mathbb{1}\{r_t = r \wedge q_{k-1} = \pi_{(t,k-1)}\} \right],$$

493 Coming to the expectation term, now they are no longer independent.

$$\begin{aligned} \mathbb{E} \left[\sum_{t=1}^{k!} \mathbb{1}\{r_t = r \wedge q_{k-1} = \pi_{(t,k-1)}\} \right] &= \sum_{t=1}^{k!} \mathbb{P}(r_t = r \wedge q_{k-1} = \pi_{(t,k-1)}), \\ &= \sum_{t=1}^{k!} \mathbb{P}(r_t = r | q_{k-1} = \pi_{(t,k-1)}) \mathbb{P}(q_{k-1} = \pi_{(t,k-1)}), \\ &= \sum_{t=1}^{k!} [\mathbb{P}(r_t = r, q = \pi_t | q_{k-1} = \pi_{(t,k-1)}) + \mathbb{P}(r_t = r, q \neq \pi_t | q_{k-1} = \pi_{(t,k-1)})] \mathbb{P}(q_{k-1} = \pi_{(t,k-1)}), \end{aligned}$$

$$\begin{aligned} \mathbb{P}(r_t = r, q = \pi_t | q_{k-1} = \pi_{(t,k-1)}) &= \mathbb{P}(r_t = r | q = \pi_t, q_{k-1} = \pi_{(t,k-1)}) \mathbb{P}(q = \pi_t | q_{k-1} = \pi_{(t,k-1)}), \\ &= 1 \cdot \frac{1}{(k-1)!} = \frac{1}{(k-1)!}. \end{aligned}$$

$$\begin{aligned} \mathbb{P}(r_t = r, q \neq \pi_t | q_{k-1} = \pi_{(t,k-1)}) &= \mathbb{P}(r_t = r | q \neq \pi_t, q_{k-1} = \pi_{(t,k-1)}) \mathbb{P}(q \neq \pi_t | q_{k-1} = \pi_{(t,k-1)}), \\ &= \frac{1}{|\mathcal{R}|} \cdot \left[1 - \frac{1}{(k-1)!} \right] \end{aligned}$$

494 Summimg them up and substituting in the previous equation, we get,

$$\begin{aligned} \mathbb{E} \left[\sum_{t=1}^{k!} \mathbb{1}\{r_t = r \wedge q_{k-1} = \pi_{(t,k-1)}\} \right] &= \sum_{t=1}^{k!} \left[\frac{1}{(k-1)!} + \frac{1}{|\mathcal{R}|} \cdot \left(1 - \frac{1}{(k-1)!} \right) \right] \frac{1}{k}, \\ &= k! \left[\frac{1}{(k-1)!} + \frac{1}{|\mathcal{R}|} \cdot \left(1 - \frac{1}{(k-1)!} \right) \right] \frac{1}{k}, \\ &= \frac{|\mathcal{R}| - 1}{|\mathcal{R}|} + \frac{(k-1)!}{|\mathcal{R}|}. \end{aligned}$$

495 Substituting this back in the expectation term, we get,

$$\begin{aligned} E \left[\sum_{t=1}^{k!} \mathbf{s}_t \mathbb{1}\{r_t = r \wedge q_{k-1} = \pi_{(t,k-1)}\} \right] &= \frac{e^{\gamma_1}}{e^{\gamma_1} + k - 1} \frac{1}{(k-1)!} \mathbb{E} \left[\sum_{t=1}^{k!} \mathbb{1}\{r_t = r \wedge q_{k-1} = \pi_{(t,k-1)}\} \right] \\ &= \frac{e^{\gamma_1}}{e^{\gamma_1} + k - 1} \frac{1}{(k-1)!} \left[\frac{|\mathcal{R}| - 1}{|\mathcal{R}|} + \frac{(k-1)!}{|\mathcal{R}|} \right], \\ &= \frac{e^{\gamma_1}}{e^{\gamma_1} + k - 1} \left[\frac{|\mathcal{R}| - 1}{(k-1)!|\mathcal{R}|} \right] + \frac{e^{\gamma_1}}{e^{\gamma_1} + k - 1} \frac{1}{|\mathcal{R}|}. \end{aligned}$$

496 Recall the term for $i \neq i$, we have,

$$\mathbb{E} \left[\sum_{t=1}^{k!} \mathbf{s}_t \mathbb{1}\{r_t = r \wedge q_{k-1} = \pi_{(t,k-i)}\} \right] = \frac{1}{e^{\gamma_1} + k - 1} \frac{1}{(k-1)!} \sum_{t=1}^{k!} \frac{1}{k|\mathcal{R}|} = \frac{1}{e^{\gamma_1} + k - 1} \frac{1}{|\mathcal{R}|}.$$

497 Note that

$$\begin{aligned}\mathbb{E} \left[\sum_{t=1}^{k!} \mathbf{s}_t \mathbb{1}\{r_t = r\} \right] &= \sum_{i=1}^k \mathbb{E} \left[\sum_{t=1}^{k!} \mathbf{s}_t \mathbb{1}\{r_t = r \wedge q_{k-1} = \pi_{(t,k-i)}\} \right], \\ &= \frac{e^{\gamma_1}}{e^{\gamma_1} + k - 1} \left[\frac{|\mathcal{R}| - 1}{(k-1)!|\mathcal{R}|} \right] + \frac{1}{|\mathcal{R}|}.\end{aligned}$$

498 Now for $i \neq 1$, we have,

$$\begin{aligned}\mathbb{E} \Delta_{1,i} &= -\mathbb{E} \left[\sum_{t=1}^{k!} \mathbf{s}_t \mathbb{1}\{r_t = r \wedge q_{k-1} = \pi_{(t,k-i)}\} - \left(\sum_{j=1}^{k!} \mathbf{s}_j \mathbb{1}\{r_j = r\} \right) \frac{1}{e^{\gamma_1} + k - 1} \right], \\ &= - \left[\frac{1}{e^{\gamma_1} + k - 1} \frac{1}{|\mathcal{R}|} - \left(\frac{e^{\gamma_1}}{e^{\gamma_1} + k - 1} \left[\frac{|\mathcal{R}| - 1}{(k-1)!|\mathcal{R}|} \right] + \frac{1}{|\mathcal{R}|} \right) \frac{1}{e^{\gamma_1} + k - 1} \right], \\ &= \frac{1}{(e^{\gamma_1} + k - 1)^2} \left[\frac{e^{\gamma_1}(|\mathcal{R}| - 1)}{(k-1)!|\mathcal{R}|} \right].\end{aligned}$$

499 Now for $i = 1$, we have,

$$\begin{aligned}\mathbb{E} \Delta_{1,1} &= -\mathbb{E} \left[\sum_{t=1}^{k!} \mathbf{s}_t \mathbb{1}\{r_t = r \wedge q_{k-1} = \pi_{(t,k-1)}\} - \left(\sum_{j=1}^{k!} \mathbf{s}_j \mathbb{1}\{r_j = r\} \right) \frac{e^{\gamma_1}}{e^{\gamma_1} + k - 1} \right], \\ &= - \left[\frac{e^{\gamma_1}}{e^{\gamma_1} + k - 1} \left[\frac{|\mathcal{R}| - 1}{(k-1)!|\mathcal{R}|} \right] + \frac{e^{\gamma_1}}{e^{\gamma_1} + k - 1} \frac{1}{|\mathcal{R}|} - \left(\frac{e^{\gamma_1}}{e^{\gamma_1} + k - 1} \left[\frac{|\mathcal{R}| - 1}{(k-1)!|\mathcal{R}|} \right] + \frac{1}{|\mathcal{R}|} \right) \frac{e^{\gamma_1}}{e^{\gamma_1} + k - 1} \right], \\ &= - \left[\frac{e^{\gamma_1}}{e^{\gamma_1} + k - 1} \left[\frac{|\mathcal{R}| - 1}{(k-1)!|\mathcal{R}|} \right] - \frac{(e^{\gamma_1})^2}{(e^{\gamma_1} + k - 1)^2} \left[\frac{|\mathcal{R}| - 1}{(k-1)!|\mathcal{R}|} \right] \right], \\ &= - \left[\frac{e^{\gamma_1}(k-1)}{(e^{\gamma_1} + k - 1)^2} \left[\frac{|\mathcal{R}| - 1}{(k-1)!|\mathcal{R}|} \right] \right] = -(k-1) \mathbb{E} \Delta_{1,i} \text{ for } i \neq 1.\end{aligned}$$

500 \square

501 D Technical Lemmas

502 **Gradient of the first layer.** For both relative positional encoding, the gradient of the first layer can
503 be computed as follows.

504 **Lemma D.1.** Denote the forward pass of the first layer as follows,

$$\mathbf{R}^h = \boldsymbol{\sigma}(\mathbf{A}^h) \mathbf{X}, \quad \mathbf{R}_t^h = \mathbf{X}^\top \boldsymbol{\sigma}(\mathbf{A}^h)_t = \sum_{i=0}^t \boldsymbol{\sigma}(\mathbf{A}^h)_{t,i} \mathbf{e}_{x_i}^s,$$

505 The gradient of the embeddings with respect to the parameters \mathbf{w}_i^h is given by

$$\frac{\partial \mathbf{R}_t^h}{\partial \mathbf{w}_i^h} = \begin{cases} \frac{e^{\mathbf{w}_i^h}}{\sum_{j=0}^t e^{\mathbf{w}_j^h}} \left(\mathbf{e}_{x_{t-i}}^s - \mathbf{R}_t^h \right) & \text{if } i \leq t, \\ 0 & \text{if } i > t, \end{cases}$$

Proof.

$$\begin{aligned}\mathbf{R}^h &= \boldsymbol{\sigma}(\mathbf{A}^h) \mathbf{X}, \\ \mathbf{R}_t^h &= \mathbf{X}^\top \boldsymbol{\sigma}(\mathbf{A}^h)_t = \sum_{i=0}^t \boldsymbol{\sigma}(\mathbf{A}^h)_{t,i} \mathbf{e}_{x_i}^s\end{aligned}$$

506 Recall that the matrix \mathbf{A}^h is defined as follows,

$$\mathbf{A}^h = \begin{bmatrix} \mathbf{w}_0^h & 0 & 0 & \dots & 0 \\ \mathbf{w}_1^h & \mathbf{w}_0^h & 0 & \dots & 0 \\ \mathbf{w}_2^h & \mathbf{w}_1^h & \mathbf{w}_0^h & \dots & 0 \\ \vdots & \vdots & \vdots & \ddots & \vdots \\ \mathbf{w}_{l-2}^h & \mathbf{w}_{l-3}^h & \dots & \mathbf{w}_0^h & 0 \\ \mathbf{w}_{l-1}^h & \mathbf{w}_{l-2}^h & \mathbf{w}_{l-3}^h & \dots & \mathbf{w}_0^h \end{bmatrix}$$

507 Now,

$$\begin{aligned} \boldsymbol{\sigma}(\mathbf{A}^h)_{t,i} &= \frac{e^{\mathbf{w}_{t-i}^h}}{\sum_{j=0}^t e^{\mathbf{w}_j^h}}, \\ \mathbf{R}_t^h &= \sum_{i=0}^t \frac{e^{\mathbf{w}_{t-i}^h}}{\sum_{j=0}^t e^{\mathbf{w}_j^h}} \mathbf{e}_{x_i}^s = \sum_{i=0}^t \frac{e^{\mathbf{w}_i^h}}{\sum_{j=0}^t e^{\mathbf{w}_j^h}} \mathbf{e}_{x_{t-i}}^s, \\ \text{For } i \leq t, \quad \frac{\partial \mathbf{R}_t^h}{\partial \mathbf{w}_i^h} &= \frac{e^{\mathbf{w}_i^h}}{\sum_{j=0}^t e^{\mathbf{w}_j^h}} \mathbf{e}_{x_{t-i}}^s - \frac{e^{\mathbf{w}_i^h}}{\left(\sum_{j=0}^t e^{\mathbf{w}_j^h}\right)^2} \sum_{j=1}^t e^{\mathbf{w}_j^h} \mathbf{e}_{x_{t-j}}^s, \\ &= \frac{e^{\mathbf{w}_i^h}}{\sum_{j=0}^t e^{\mathbf{w}_j^h}} \left(\mathbf{e}_{x_{t-i}}^s - \mathbf{R}_t^h \right) \end{aligned}$$

508 So, we have the result as follows,

$$\frac{\partial \mathbf{R}_t^h}{\partial \mathbf{w}_i^h} = \begin{cases} \frac{e^{\mathbf{w}_i^h}}{\sum_{j=0}^t e^{\mathbf{w}_j^h}} \left(\mathbf{e}_{x_{t-i}}^s - \mathbf{R}_t^h \right) & \text{if } i \leq t, \\ 0 & \text{if } i > t, \end{cases}$$

509 □

510 Now in the context of simplified transformer model with a fixed window we have the following

511 **Lemma D.2.** Denote the forward pass of the first layer as follows,

$$\mathbf{R}^h = \boldsymbol{\sigma}(\mathbf{A}^h) \mathbf{X}, \quad \mathbf{R}_t^h = \mathbf{X}^\top \boldsymbol{\sigma}(\mathbf{A}^h)_t = \sum_{i=1}^k \boldsymbol{\sigma}(\mathbf{A}^h)_{t,t-i} e_{\pi_{(t,k-i)}},$$

512 The gradient of the embeddings with respect to the parameters \mathbf{w}_i^h is given by

$$\frac{\partial \mathbf{R}_t^h}{\partial \mathbf{w}_i^h} = \frac{e^{\mathbf{w}_i^h}}{\sum_{j=1}^k e^{\mathbf{w}_j^h}} \left(e_{\pi_{(t,k-i)}} - \mathbf{R}_t^h \right)$$

Proof.

$$\mathbf{R}^h = \boldsymbol{\sigma}(\mathbf{A}^h) \mathbf{X}, \quad \mathbf{R}_t^h = \mathbf{X}^\top \boldsymbol{\sigma}(\mathbf{A}^h)_t = \sum_{i=1}^k \boldsymbol{\sigma}(\mathbf{A}^h)_{t,t-i} e_{\pi_{(t,k-i)}},$$

$$\sigma(\mathbf{A}^h)_{t,t-i} = \frac{e^{\mathbf{w}_i^h}}{\sum_{j=1}^k e^{\mathbf{w}_j^h}},$$

$$\mathbf{R}_t^h = \sum_{i=1}^k \frac{e^{\mathbf{w}_i^h}}{\sum_{j=1}^k e^{\mathbf{w}_j^h}} e_{\pi_{(t,k-i)}},$$

$$\text{For } 1 \leq i \leq k, \quad \frac{\partial \mathbf{R}_t^h}{\partial \mathbf{w}_i^h} = \frac{e^{\mathbf{w}_i^h}}{\sum_{j=1}^k e^{\mathbf{w}_j^h}} (e_{\pi_{(t,k-i)}} - \mathbf{R}_t^h)$$

□

515 E Additional Experiments

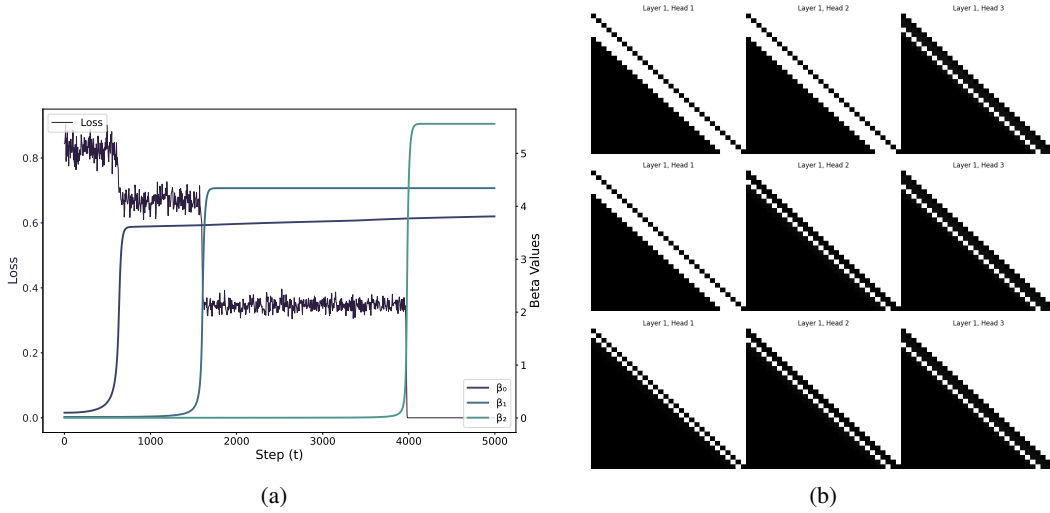


Figure 4: The left panel is shown in **a** and the right panel in **b**. Note that the β values rise as the loss drops, and the attention patterns at times 800, 1750, and 4500 demonstrate incremental learning. This is in the opposite order as they are initialized in the opposite order $\beta_3 > \beta_2 > \beta_1$